AN ANALYSIS OF THE ENERGETICS AND STORMWATER MEDIATION POTENTIAL OF GREENROOFS

by

ROGER N. HILTEN

(Under the Direction of E. W. Tollner)

ABSTRACT

A study was conducted to examine the effects induced by a greenroof installation on a typical roof in various climate types of the United States. Initially, heat and moisture transport parameters of a modular greenroof system were evaluated based on physical measurements and simulated soil hydraulics. Using climatic data, the greenroof system was then evaluated to determine the stormwater runoff reduction potential compared to a BUR (Built-Up Roof) and overall energy load effects compared to a BUR and a reflective, "cool" roof in seven U.S. evaluation cities. Runoff simulations were run in HYDRUS-1D, while energy load simulations were run for a hypothetical office building in the evaluation cities using eQuest, a DOE-developed building energy load simulation. Simulation results were validated based upon *in situ* observations at a greenroof installation in Athens, Georgia. Simulated runoff and cooling load reductions for the evaluation cities ranged from 17-81 % and 2.5-6.9 %, respectively.

INDEX WORDS: greenroof, engineered soil, evapotranspiration, heat transport, moisture transport, multi-climate, micrometeorology, building energy

AN ANALYSIS OF THE ENERGETICS AND STORMWATER MEDIATION POTENTIAL OF GREENROOFS

by

ROGER N. HILTEN

B.S., University of Georgia, 2002

A Thesis Submitted to the Graduate Faculty of The University of Georgia in Partial Fulfillment of the Requirements for the Degree

MASTER OF SCIENCE

ATHENS, GEORGIA

2005

AN ANALYSIS OF THE ENERGETICS AND STORMWATER MEDIATION POTENTIAL OF GREENROOFS

by

ROGER N. HILTEN

Major Professor: William Tollner

Committee: Thomas Lawrence
David Gattie

Electronic Version Approved:

Maureen Grasso
Dean of the Graduate School
The University of Georgia
December 2005

DEDICATION

I dedicate the following work to my ever-supportive wife, Annie, and mentor, Amy Rosemond, each for revealing unseen opportunities and believing in me.

ACKNOWLEDGEMENTS

I thank St. Louis Metalworks Company for graciously donating the greenroof blocks for the study presented herein. Also, the University of Georgia Agricultural Experiment Station for providing financial support for the project.

I also adamantly thank Tom Lawrence for providing indispensable guidance and advice throughout the duration of the project. Dr. Lawrence's contributions were essential to the completion of the project. I also acknowledge E.W. Tollner, David Gattie and David Stooksbury whose comments have been instrumental in guiding the direction of the work.

In addition, I acknowledge Todd Rasmussen and David Radcliffe for their assistance and technical support for the greenroof monitoring and modeling portions of the research. Finally, I thank fellow graduate students Tim Carter and Eric Prowell for their contributions of data and moral support for the project.

TABLE OF CONTENTS

Page

LIST OF TABLES

Page

LIST OF FIGURES

Page

CHAPTER 1

INTRODUCTION

Background

Vegetation has been utilized in urban roof construction for thousands of years for both aesthetics and function. Examples range from the ancient hanging gardens of Babylon (Liu, 2002) to modern roof gardens in large cities throughout the world. In Germany alone, over 145,000,000 square feet of roof space are now covered with some sort of vegetation (Herman, 2003; Markum and Walles, 2003). Here in the U.S., green roofing has yet to reach such proportions. However, several cities in the U.S. including Chicago, IL and Portland, OR now offer tax incentives to building owners who opt to install greenroofs roofs in an effort to reduce stormwater runoff. With the proliferation of greenroofing comes vital need for a fuller understanding of the effects of greenroofs.

The modern practice of incorporating vegetation into roof construction, known as green roofing, comes in myriad variations, but all types evoke similar benefits. Despite a broad range of cited benefits, green roofing currently has been incorporated into structure design more as a qualitative, aesthetic addition to structures (Theodosiou, 2003). However, in addition to aesthetic enhancement of buildings, other widely cited functional benefits include; sound insulation, stormwater detention, roof protection, urban heat island reduction and improved thermal performance for cooling and heating load reductions (Del Barrio, 1998; Markum and Walles, 2003). Quantitative evidence of benefit in areas of stormwater mediation and thermal performance is integral in garnering acceptance of greenroofing in the United States.

Consequently, the current research focuses on stormwater mediation potential and thermal performance of greenroofs in U.S. climates.

Intent and Structure of Current Research

The current research attempts to elucidate the effects of greenroofs on stormwater runoff and building energy loads in multiple U.S. climates compared to conventional roof types. Since little research has been conducted on greenroofs in the U.S. compared to the European Union, such studies are needed to describe the effects of adding a vegetative layer to a building envelope. The research outlined herein includes field site and laboratory studies as well as two simulation studies. The goal of the research was to develop a predictive tool for designers and builders to use to assess the benefits of greenroofs for any build site where climate data is available.

Thesis structure

The following thesis is constructed in "Manuscript" style. Three separate chapters correspond to three journal articles soon to be submitted. Chapter Two, the first manuscript, describes a method devised to determine stormwater runoff from a modular block greenroof system in each of the evaluation cities of Table 1.1. Simulation inputs were obtained from both field and laboratory studies. Chapter Three describes the portion of the overall study involving the estimation of thermal conductivity of a previously untested engineered greenroof soil. Estimation methods incorporated both simulated and measured quantities. Finally, the study outlined in Chapter Four compiled results from studies of the previous two chapters in order to simulate building energy loads for greenroof sited in each evaluation city.

Field studies

The field portion of the study took place on the University of Georgia's Science Library, where an extensive modular block greenroof system was installed during August of 2004. The greenroof system, donated to the University of Georgia by Green Roof Blocks, a subsidiary of St. Louis Metalworks Company, consisted of 100 two foot by two foot square aluminum pans, or blocks, at four inches deep. Each block held approximately four inches of engineered greenroof soil vegetated with five species of *Sedum* a succulent stonecrop. *Sedum* species included spp. reflexum, sexangulare, immegrauch, spurium, and album.

With automated atmospheric and soil monitoring equipment, measurements were obtained and used to calculate evapotranspiration by the Food and Agricultural Organization's standardized method based on the combination equation of Penman-Monteith (Penman, 1948; Monteith, 1965; De Bruin and Holtslag, 1982), described in detail in Chapter Two. In addition, soil parameter measurements were taken in order to calculate thermal conductivity for the engineered soil of the study site. Observed thermal conductivity was used to validate three conductivity estimation methods including those of De Vries (1966), Vershinin (1966), and Campbell (1985), which are based on physical properties of the soil. Once validated, the estimation methods were used to predict an average yearly thermal conductivity for each of seven evaluation cities shown in Table 1.1 to be used in a DOE-developed building energy modeling program, eQuest (QUick Energy Simulation Tool)(James J. Hirsch, 2005).

At an adjacent site, a separate study observed greenroof block runoff, where runoff in this case was considered water that has infiltrated the engineered soil and exited the blocks' drains. The separate ongoing runoff study is being conducted by Eric Prowell, a graduate student in the

Table 1.1. Evaluation cities with climate type and average seasonal weather conditions

City	Climate Type	Temperature* (C)		Monthly Rainfall (cm)	
		Summer	Winter	Summer	Winter
Atlanta	moist warm-temperate	30/19	14/3	10.4	10.5
Denver	grassland (steppe)	28/12	8/-7	5.0	1.6
Honolulu	tropical	30/23	27/20	1.6	7.6
Los Angeles	summer-dry, winter wet	24/16	20/10	0.2	6.0
New York	cool-temperate	27/18	7/0	11.0	10.7
Phoenix	semidesert	39/24	21/7	1.3	1.9
Seattle	cool-temperate	22/11	9/3	3.2	13.7

Climate type adapted from Aber and Melillo, 1991.
*High/Low. Climate data from NOAA 30-yr normals for Nov-Feb and Apr-Aug

University of Georgia's Forestry Department. Data sharing between researchers has allowed a validation parameter for the stormwater simulations used in the current research.

Laboratory studies

In addition to field-measured quantities, certain soil specific parameters were determined by a laboratory experiment. Lab measured parameters consisted predominantly of hydraulic properties of the engineered soil, which were not available in the literature. More specifically, a characteristic moisture release curve was constructed for the soil, which describes the volumetric moisture content of a soil at varying pressure heads. From this curve, both residual and saturated moisture content of the soil were estimated. The purpose of the laboratory study was to obtain required parameters for a soil moisture transport simulation, namely HYDRUS-1D, a heat, moisture and multiple solute transport simulation for variable-saturated porous media.

Simulations

Two packaged simulations were used in the current study, one to predict soil hydraulic properties and stormwater runoff, and the other to predict building energy loads. Both simulations were used to obtain estimates for each of the seven evaluation cities of Table 1.1. Essentially, the goals of both the field and laboratory study were to obtain parameters to be input to simulations in order to obtain runoff from HYDRUS-1D and building energy loads from eQuest.

Of the simulations, the first, HYDRUS-1D, was used to predict stormwater runoff from a modular block greenroof for a given year, 2004 in this case, for each of the evaluation cities. This portion of the study is described in detail in Chapter Two. HYDRUS' stormwater simulations required inputs of soil hydraulic parameters (obtained during laboratory study) in addition to evapotranspiration and rainfall obtained from 2004 National Weather Service Climate Data. Runoff comparisons were made between greenroof blocks and an impervious roof for greenroof soil depths; five, ten (as in study site), fifteen, and thirty centimeters. For the impervious roof, all rainfall striking the equivalently sized roof was assumed to be runoff. Validation of the HYDRUS simulation was obtained via comparison to measurements taken at the Athens site runoff study.

For the building energy simulations in eQuest, a prediction of thermal conductivity, described in Chapter Three, was first required. In order to obtain thermal conductivity in the evaluation cities, HYDRUS was again used, in this case as a prediction tool for soil moisture content, a dominant parameter in thermal conductivity functions. In order to validate soil moisture predictions, study site parameters were first input to HYDRUS, and soil moisture content acquired was compared to the actual site measured quantity. Upon validation, soil

volumetric moisture content was then predicted for each evaluation city. In eQuest, building energy loads are simulated with environmental forcings derived from TMY (Typical Meteorological Year) data. Therefore, to assess thermal conductivity for these simulations, TMY data was also used in HYDRUS to predict soil moisture in the evaluation cities.

The process of obtaining thermal conductivity, outlined in Chapter Three, involved the HYDRUS output, soil volumetric moisture content, for the seven evaluation cities. From this output, thermal conductivity was predicted by three methods including those of De Vries (1966), Vershinin (1966), and Campbell (1985) from which an average was taken for the year to be input to eQuest. In addition to soil moisture, thermal conductivity models generally required an estimate of density and volumetric heat capacity, which were each observed in the laboratory experiment. Actual thermal conductivity of the soil was assessed using Fourier's steady-state heat conduction equation using measured quantities at the study site at six am when the system was assumed to be at steady state. Estimated thermal conductivity as a function of soil moisture computed via De Vries, Vershinin, and Campbell was validated based on the actual thermal conductivity measured on site.

The second simulation process using eQuest, outlined in Chapter Four, incorporated quantities including thermal conductivity and volumetric heat capacity previously assessed in Chapters Two and Three to determine building energy loads. A standard office building was designed in eQuest with one of three roof covering types; a reflective, or "cool", roof, an extensive modular block greenroof, or a BUR (Built-Up Roof). Several variations of these types were simulated as well. For the study site city, Athens, GA, loads were determined for three building heights (one, three, and eight stories) each with two equally sized (929 m^2) building footprint shapes (square and rectangular). The intent of simulating different height and shaped

buildings was to determine at what point the effects of roof type become negligible. In addition, building energy loads were predicted for each evaluation city. For one city in particular, Seattle, WA, three additional greenroof soil depths, five, fifteen, and thirty centimeters, along with the ten-centimeter greenroof of the study site were simulated. Chapter Four describes the results of the building energy modeling.

Literature Review

The following review is separated into three separate sections describing articles corresponding to greenroof thermal analysis, thermal analysis of soils, and stormwater analysis.

Greenroof thermal analysis studies

It is well known that vegetated roof coverings, or greenroofs, can lower rooftop surface temperatures in warm climates (Del Barrio, 1998, Niachou, 2001, Liu, 2002, and Theodosiou, 2003). The magnitude of temperature reduction and resulting reduction of heat flow into structures is dependent upon many factors associated with a greenroof's construction and with the climate of the area. However, preliminary research at the University of Georgia reveals that at an ambient air temperature of 298 Kelvin (25 ºC), green roof surface temperature at the roof's outer structural skin is approximately 10 K (10 ºC) cooler than an adjacent non-vegetated roof. At 308 K (35 ºC), the temperature difference reaches 25 K (25 ºC) (unpublished data). Researchers ascribe cooler surface temperatures to evaporation, transpiration, and shading effects (Del Barrio, 1998 and Liu, 2002). Cooler surface temperatures translate to decreased heat transfer through roofs into occupied space thereby reducing cooling loads in warm months. Cooling load reduction is an important selling point for green roofs.

Previous research has focused primarily on the potential of greenroofs as passive cooling devices. Therefore, research has generally been focused on warm, dry climate effects (Del

Barrio, 1998, Theodosiou, 2003 and Niachou et al, 2001) where evaporative cooling potential is high, though sparse rainfall limits moisture availability for evaporation. A much smaller collection of research has been conducted to assess greenroof effects in cooler seasons or climates or in moist conditions, where moisture needed for passive cooling is available. Though studies exist for diverse climate types, none do so concurrently to compare economic gains. Thermal analysis studies reviewed in current research observe climate types including cool, temperate grassland (Liu, 2003), tropical (Wong et al., 2003), and Mediterranean (Niachou et al, 2001 and Theodosiou, 2003). Though these climate types exist in the U.S., currently, most green roof installations are in other climatic areas.

Without a multi-climate green roof model that reveals performance characteristics for a specific geographical site, building designers may find green roofs to be a difficult sell to stakeholders. Therefore, this thesis develops a model to predict green roof passive cooling and insulating potential under multiple climate regimes. With this model, designers can gather and assess information as to the benefits and costs associated with green roofing in their areas.

In both cool and humid climates, evaporative potential limits the cooling effects transpiration and evaporation provide. However, in a study conducted in Singapore (wet, tropical conditions), Wong et al (2003) have observed that vegetation can consume solar heat gain through evapotranspiration and photosynthesis. This consumption of solar heat implies that passive cooling is occurring. In cooler areas, other parameters including thermal mass may become significant factors in determining green roof thermal performance, where performance in this case is equated with heating load reduction. A limited number of studies have observed green roof effects in winter months with Liu (2002) being the exception. Despite the lack of study, Del Barrio (1998) predicts that soil moisture, a thermal mass contributor, may be the

essential factor in the insulating capacity of green roof systems in winter. For that reason, the study also assessed green roofs' insulating capacity in winter.

In order to determine the effects of various roof coverings on building energy loads, several mathematical and empirical models are required. Several articles cited in this review lay groundwork for the current research. However, the first section of the review cites articles that actually use the various models to assess the energy-saving potential of roof systems.

In the first article, Del Barrio (1998) utilizes a mathematical model yielding a sensible, albeit simplified representation of the dynamic thermal behavior of actual green roofs. Del Barrio incorporates parametric sensitivity analyses to determine green roof variables that most affect the cooling potential in summer months. Driving variables include the leaf area index (LAI) and the foliage geometrical characteristics, the soil apparent density, thickness, and moisture content. In her study of green roofs in a Mediterranean climate, Del Barrio utilizes several fundamental equations to be used in the current proposed research. Most importantly, one empirically derived equation for soil conductivity outlined by Del Barrio will be utilized.

In her analyses, Del Barrio concludes that green roofs do not act as cooling devices but as insulation that merely acts to reduce the heat flux through the roof. However, a cooling effect is still possible in locations other than the Mediterranean, where dry, hot climate conditions excessively dry greenroof soil reducing evaporative surface cooling. Del Barrio (1998) derives and defines many of the governing equations, and determines several assumptions in the model that help to simplify calculations. For the soil portion, these assumptions include: (1) fluxes are one dimensional, (2) the soil is homogenous and isotropic, (3) liquid and vapor phases of water are in equilibrium, and (4) soil pore sizes are small so subsurface convection is negligible.

Del Barrio defines three distinct mathematical models; one for the roof support structure, one for the soil system, and one for the canopy. Del Barrio's canopy model will also be utilized for the proposed study. This model outlines the main canopy processes including: 1) solar radiation absorbed by leaves; 2) longwave radiation exchanges between leaves and sky, ground, and other leaves; 3) convective heat transfer between leaves and canopy air, and between ground and canopy air; 4) evapotranspiration in leaves; 5) evaporation and condensation of water vapor in soil surface and vapor convective transfer between the soil surface and the air; 6) convective heat and vapor transfer between the air in the canopy and free air.

Theodosiou (2003) and Niachou et al (2001) each describe green roof effects in Mediterranean climates. In Mediterranean climates where wet winters and dry summer conditions dominate, Theodosiou asserts that planted roofs not only insulate, but also can provide passive cooling for building interiors via evaporative cooling. Both articles develop a simulation model to describe the thermal behavior of roof systems topped with vegetation, then compare simulation output to empirical observations from an existing green roof in the Mediterranean area.

Another method of reducing building energy loads consists of altering the solar reflectivity of the roof surface. For example, by increasing the reflectivity, sun-derived thermal radiation that is transmitted to roof surfaces is reduced. With this in mind, Akbari (2003) observed the effects of altering the solar reflectivity of two small non-residential buildings. After applying a reflective white coating to each building, Akbari (2003) determined the cooling load reductions the buildings experienced. By increasing roof surface reflectivity (albedo) from 26-72% using the alternate coating, the study reported savings of $\$0.86/m^2$ per year in cooling costs.

Incorporating solely empirical measurements, a study by the National Research Council Canada by Liu (2002) evaluates the performance of a planted roof in Ottawa, Canada. For a generic planted roof and a BUR, a baseline temperature comparison was made at the roof's waterproof membrane layer. Liu found that median daily temperature fluctuations for planted and conventional roof were 6.5 and 46 °C, respectively. Assuming equal amounts of incoming long and shortwave radiation for the two roof assemblies, Liu shows that lowering membrane temperatures reduces heat flow through the study's building envelope. The article attributes lower membrane temperatures to direct shading from vegetation, evaporative cooling, and additional insulation values afforded by plants and soil.

Wong et al (2003) observed the thermal impact of a rooftop garden in Singapore, a tropical environmental. The study found that rooftop vegetation caused a negative heat flux (removal of thermal energy from the underlying building) during most of the day compared to a positive, downward heat flux (addition of thermal energy to underlying building) for an adjacent bare roof. For certain vegetation types such as shrubs, a negative heat flux was always observed. This is an important observation given that none of the studies conducted in Mediterranean areas (Del Barrio, 1998, Theodosiou, 2002, and Niachou, 2001) revealed similar passive cooling capabilities. In addition, Wong showed that insulating capability was defined by soil and was not substantially affected by vegetation.

Literature Review - Soil thermal modeling

The second set of papers outlines the fundamental equations required to assess the performance a greenroof, several of which were utilized in the greenroof studies previously mentioned. Many of the fundamental equations in the following studies involve the theory and

methods for determining heat and moisture transfer parameters for a given soil/plant/atmosphere continuum.

The first, and perhaps most important, parameters relate to the greenroof soil's ability to transfer thermal energy. A dominant portion of the current study depends on accurate estimation of soil thermal characteristics including thermal capacity and conductivity. Estimating the thermal conductivity of the greenroof system requires intimate knowledge of the soil's physical composition and water content. Although the characteristics of many naturally occurring soils have been well documented in literature, few studies observe greenroof soils. Often, greenroof soils are specifically engineered to perform in predictable ways. The current study required both a method to predict soil thermal conductivity on site and also to predict the parameter in other locations. The following portion of the literature review outlines the models used to estimate soil thermal conductivity and the models' respective parameter requirements.

In De Vries (1966), a data intensive method for determining thermal conductivity, hence called the De Vries method, is described in great detail. Generally, the method is based on the theory of thermal conductivity of granular materials with particular emphasis on soils. This model takes as input the individual specific heat values and relative volumetric fraction for each soil constituent. The soil's volumetric heat capacity is then merely a linear function calculated as the summation of each constituent's specific heat multiplied by its density and volumetric fraction. Soil constituents include solid, water, and air fractions, for which the solid fraction can be separated to quartz, organic matter, and "other minerals" fractions. The air fraction is usually neglected due its low density and hence low volumetric heat capacity compared to other soil constituents.

Obtaining thermal conductivity using the De Vries method relies on the theory of thermal conductivity for granular materials. For soils, shape factors are assigned to soil granules based on the ratios of the axes of the ellipsoid soil particles. A ratio of the average temperature gradient in the soil granules is then obtained. With these soil- and time-specific values, thermal conductivity value can be estimated. However, the thermal conductivity value ignores the influences of moisture movement in the soil. Luckily, the De Vries method provides additional methodology for expressing the apparent thermal conductivity, which is a combination of the thermal conductivity due to normal heat conduction and the part due to vapor movement. Acquiring thermal conductivity due to vapor movement requires additional parameters including relative humidity in soil pores, the latent heat of vaporization, the gas constant for water vapor, the diffusion coefficient of water vapor in air, atmospheric pressure, and the saturation vapor pressure.

Another model of thermal conductivity is presented by Campbell (1985) that uses volumetric fractions of major soil constituent fractions including organic matter, quartz, other minerals, water, and clay. The fractions are combined in an empirical correlation introduced by McInnes (1981) acquired by curving fitting that gives accurate thermal conductivity values for a range of soil types.

In the next article, Vershinin (1966) describes a simple model to estimate soil thermal conductivity. Vershinin uses a simplified version of De Vries method for obtaining volumetric heat capacity that incorporates just one solid phase and the liquid phase for the estimate along with apparent density. Similar to the Campbell method, an empirical correlation is utilized to estimate soil thermal conductivity.

Literature Review – Stormwater and evaporation

Aside from the thermal energy effects of greenroofing, greenroofs provide a certain degree of perviousness to a normally impervious roof surface. In affect, an additional benefit imposed by greenroofing is detention of rainfall, which reduces stormwater runoff. The next section reviews articles related the stormwater and factors affecting the ability of greenroofs to reduce stormwater.

Stormwater mediation in the U.S. is currently a hot topic. As urbanization increases the imperviousness of watersheds, the volume of stormwater reaching streams has increased exponentially as have the pollutants that stormwater conveys. Traditionally, stormwater has been conveyed to storm sewers and stream channels as quickly as possible (Booth and Jackson, 1997, Carter and Rasmussen, 2005). However, quick conveyance translates to a high-energy flow of stormwater runoff, which can degrade geomorphology of aquatic systems via stream channelization and bank erosion (Booth and Jackson, 1998, Paul and Meyer, 2001). Such streambed alterations often make the physical environment less desirable for native stream flora and fauna (Booth and Jackson, 1998). In addition, increased temperatures of and pollutants in urban runoff limit the ability of stream biota to thrive as decomposition rates increase. As urbanization encroaches upon more aquatic systems, the need to mitigate runoff is dire.

Accordingly, in 1990 as an amendment to the Clean Water Act, the U.S. Environmental Protection Agency (EPA) established the National Pollutant Discharge Elimination System (NDPES), a stormwater permitting program, designed to limit the amount of pollutants entering municipal storm sewers from medium and large cities (greater than 100,000 and 250,000, respectively) cities and industrial sites (Harrison and Stribling, 1995). Greenroofs provide urban

planners a tool to use as part Best Management Practice's (BMP's) to retain rainfall that would normally become urban stormwater runoff.

Several factors related to moisture flux affect the ability of green roofs to mitigate urban runoff. Macroscopic moisture flux for greenroofs occurs by evaporation, transpiration, precipitation, and bottom flux (technically, deep percolation). Evaporation, transpiration, and bottom flux depend on the rate and overall depth of precipitation. Several studies (Carter and Rasmussen, 2004, Moran et al, 2005) show that retention depends strongly on the quantity of rainfall per storm event. Carter and Rasmussen (2005) observed that for an extensive greenroof site, retention decreases from 90 % for a 0.5 inch storm to 39 % for a 2.12 inch storm. The previous study also predicts that once a greenroof's field capacity is reached during a rain event, all rainfall exits as bottom flux from the greenroof soil column, and the subsequent hydrograph mimics that of an impervious roof. Field capacity depends directly on the physical characteristics of the soil media.

The amount of moisture in the soil prior to a rainfall event determines how much more moisture is required to reach field capacity. Soil moisture in the absence of rainfall changes due to evaporative fluxes. Computational methods for evapotranspirative flux in the current research rely heavily upon standardized crop water requirement methods developed by the FAO (Food and Agricultural Organization of the UN). Described by Allen et al (1998), the method known as the FAO Penman-Monteith method gives a detailed explanation for estimating crop evapotranspiration. Based on the Penman-Monteith combination equation, the FAO Penman-Monteith method utilizes commonly available weather data and specific parameters related to the crop in question to estimate evapotranspiration.

Generally, the FAO Penman-Monteith uses the 'K_c-ET_O' approach for evaporation, where evapotranspiration for a reference crop, ET_O, is estimated. The reference crop most resembles an actively growing, well-watered, extensive surface of green grass of uniform height (~ 0.12 m). Combining ET_O with K_c, crop specific coefficient, the K_c-ET_O approach calculates evapotranspiration for a specific crop, ET_C, while accounting for all the physical and physiological differences between the specific and reference crops. However, for the greenroof 'crop', in this case *Sedum*, no K_c coefficient is available. Not surprisingly, Allen et al also provides a method to determine the ET_C when several important crop parameters are known or can be estimated. These parameters include canopy resistance, aerodynamic resistance, and surface albedo. Other parameters used for the calculation of ET_O and ET_C include net radiation, air temperature, wind speed, humidity, and soil heat flux from which, several other values are calculated.

A method to predict moisture flux due to deep percolation was also required during the study. Accordingly, a combined heat, moisture, and multiple solute transport simulation, documented by Šimůnek et al (1998), was utilized in the study to predict deep percolation. HYDRUS-1D, version 2.0 is actually a software package containing HYDRUS (v.7.0) along with HYDRUS1D, a graphics-based user interface. Using the Richards' equation for variably-saturated water and convection-dispersion type equations, HYDRUS 7.0 numerically solves heat and moisture transport for a given soil (Šimůnek et al, 1998).

CHAPTER 2

PREDICTING STORMWATER RUNOFF FROM A MODULAR BLOCK GREENROOF SYSTEM WITH ENGINEERED SOIL[1]

[1] Hilten, R. N., T. M. Lawrence, and E. W. Tollner. To be submitted to the *Journal of Hydrology*.

Abstract

A study was conducted to determine how green roofing affects stormwater runoff from a rooftop. Stormwater runoff was simulated in seven evaluation cities representing various climate types of the United States. Simulations were run using HYDRUS-1D, a one-dimensional heat, moisture, and multiple solute simulation for variably-saturated porous media. Simulated runoff quantities were validated based on physical measurements at a greenroof study site located on the University of Georgia's Athens campus. The study site consisted of a 400 ft^2 modular greenroof system atop a utility room for University of Georgia Science Library. The modular blocks were 60 cm square, 10 cm deep aluminum containers filled with an engineered soil. Vegetation consisted of several *Sedum* species, a succulent CAM plant. Soil hydraulic parameters including a characteristic moisture release curve were evaluated for the engineered soil using both physical measurements from Tempe cell experiment and simulation results from HYDRUS-1D. Using 2004 climate data from seven evaluation cities along with hydraulic parameters of the greenroof soil, HYDRUS-1D predicted urban stormwater reduction in the range of 17-81 % for greenroof installations in the seven evaluation cities using a five, ten, fifteen, and thirty-centimeter soil depths.

INDEX WORDS: greenroof, engineered soil, evapotranspiration, stormwater, runoff, moisture transport, multi-climate, micrometeorology

Introduction

Green roofing in some form has been in use for thousands of years. Examples range from the hanging gardens of ancient Babylon, to sod roofing in the American west, to the modern, extensive engineered green roof systems. In the United States, interest has just begun to pique, and installations are appearing in varying environments including Michigan, Illinois, California, Georgia, Utah, and many others. The specific purposes of greenroof installations vary, but generally hinge upon stormwater reduction or improved building energy efficiency and often both. In the realm of stormwater reduction, understanding the fate of precipitation in a soil/plant/atmosphere continuum such as greenroof system is important in order to assess the stormwater mediation effectiveness of green roofing in various locations. Assessing effectiveness requires specific knowledge of each partition of the continuum.

For soils, accurate estimates of hydraulic properties are an essential requirement for predicting the fate of stormwater. For the engineered media in the current study, few studies have evaluated hydraulic properties. To derive hydraulic properties including saturated and residual hydraulic conductivity of soils, pressurized Tempe cells can be used to develop a moisture release curve for a given soil, which charts moisture content as a function of pressure head. Alternately, simulations can predict the release curve based on observed or measured values of a soil's volumetric moisture content at field capacity and wilting point. For greenroof systems, moisture fluxes are relatively easy to measure or predict with the aid of modern automated monitoring equipment. However, measurements such as runoff are not generally available for sites other than the researcher's study site. Therefore, simulations are required to predict these quantities. With measurements of rainfall and estimates for evapotranspiration,

software packages such as HYDRUS-1D can easily predict runoff. Simulated runoff can then be verified by comparing to experimental values obtained at the greenroof site.

HYDRUS-1D, version 2.0 is actually a software package containing the core program HYDRUS (v.7.0) along with HYDRUS1D, a graphics-based user interface. Using the Richards' equation for variably-saturated water and convection-dispersion type equations, HYDRUS 7.0 numerically solves heat and moisture transport for a given soil (Šimůnek et al, 1998).

The current study develops a one-dimensional, combined heat and moisture model using HYDRUS-1D, for a homogenous, engineered green roof soil. In parameter estimation mode, HYDRUS-1D estimates soil hydraulic properties and stormwater runoff based on user inputs of various soil properties and estimates of evaporation, transpiration and rainfall. Observations, micrometeorological and soil-specific, required by HYDRUS were collected at a modular block greenroof installation on the University of Georgia's Athens campus. Once the meteorological and soil parameters were input to HYDRUS, runoff volumes were obtained and verified by comparing to actual runoff from the greenroof blocks.

Upon verification of HYDRUS-derived stormwater runoff, evaporation values calculated from 2004 climate data from seven evaluation cities were entered to HYDRUS to determine the percent reduction in volume afforded by modular block greenroofs compared to conventional, impervious roofs. Such knowledge could help builders, designers and planners determine the effectiveness of green roofing as an urban stormwater mediation technique.

Materials and Methods

The study site

The study site consisted of one hundred square aluminum green roof blocks with dimensions, 60 x 60 x 10 cm, donated to the University of Georgia by Green Roof Blocks, a

subsidiary of St. Louis Metalworks Company. Each block is filled with approximated 10 cm of engineered soil (80% expanded slate, 20% organic matter) with density of approximately 900 kg m^{-2}. Each soil block is vegetated with one of five species of *Sedum*, a low-lying succulent stonecrop. *Sedum* species included, spp. reflexum, sexangulare, immegrauch, spurium, and album.

Measurements

In situ measurements were collected from January to August of 2005. Measurements included the micrometeorological parameters; humidity (0.15 and 1.1 m above surface), air temperature (0.15 and 1.1 m), windspeed (1.2 m), radiation (net, solar, and photosynthetically-active), and soil parameters including soil temperature (0.0, 0.045, and 0.09 m below surface), volumetric moisture content, and heat flux. Automated measurements were taken every fifteen minutes as averages of values sampled every ten seconds.

Runoff collection was measured at an adjacent site at which similar modular green roof blocks were mounted atop collection bins fitted with pressure transducers connected to an automated datalogger to record bin water depth every two minutes starting at the outset of a storm event (Prowell, pers comm.).

Laboratory experiments

In addition to site measurements, a laboratory experiment was conducted to evaluate the characteristic moisture release curve for the engineered greenroof soil using pressurized Tempe cells. The curve describes the volumetric moisture content of a soil versus pressure head. Applied pressures at 33 and 1500 kPa correspond to the soil's field capacity and wilting point moisture content, respectively. Tempe cells of known volume were packed with intact green roof soil cores, and then were fully saturated using a 0.01 M calcium chloride solution. The cells

were then enclosed in a pressure chamber with a selectively permeable ceramic bottom plate. Various pressures (1, 3, 9, 19, 33, 75, and 1500 kPa) were applied to a valve on the tops of the pressure chambers. Each pressure setting was maintained until equilibrium was reached at which point the weight of each cell no longer fluctuated. Weight was then recorded and the next pressure setting was applied. Once the last pressure setting was applied and equilibrium was reached, soil samples were oven dried and reweighed to determine the mass of water. From the weights observed, gravimetric moisture content at each pressure head were calculated by:

$$w = \frac{mass_{water}}{mass_{soil,od}} \tag{1}$$

where w gravimetric water content [kg m^{-3}],

$mass_{water}$ ($mass_{soil,wett} - mass_{soil,od}$) [kg],

$mass_{soil,od}$ mass of oven-dried soil [kg].

Equation 1 was used to determine gravimetric water content at each of the prescribed pressure settings. Volumetric water content was then determined by:

$$\theta = w\frac{\rho_b}{\rho_l} \tag{2}$$

where θ volumetric water content [m^3 (water) m^{-3} (soil)],

ρ_b soil bulk density [kg m^{-3}],

ρ_l density of water [kg m^{-3}].

Again, water content was computed for each of the pressure settings but this time as a volumetric fraction. Using pressure settings versus volumetric water content, a characteristic curve for the green roof soil was then plotted. With volumetric water content plotted on a log scale on the x-axis, the characteristic s-shape curve was evident. The upper portion (lower pressure) was assumed to be approaching θ_s, the saturated water content, and the lower region (higher pressure) approaching θ_r, the residual water content, of the soil.

Moisture fluxes in the green roof system

Several modes of water flux were observed or estimated in the green roof study. Generally, fluxes of moisture enter or leave the surface through soil or plant stomata, or leave through the green roof block drains. In order to satisfy conservation of mass, all moisture must be accounted for either as an incoming, outgoing or as a change in soil water storage. Once moisture leaves the green roof blocks' drains, it can be considered runoff that must be contained and routed just as if no green roof installation were present. The goal of the study was to determine the percent reduction of runoff volume associated with green roofing compared to impervious roof types.

The water balance

Understandably, accurate estimates of moisture fluxes are required in order to assess the potential of green roofing to reduce urban stormwater. Moisture fluxes occur by several means, their sources obvious when considering the following soil water balance equation, which evaluates fluxes by depth equivalent (volume of moisture divided by flux surface area):

$$I - ET + P - RO - DP + CR \pm \Delta SF \pm \Delta SW = 0 \quad (3)$$

where I irrigation [mm],

ET evapotranspiration [mm],

P precipitation [mm],

RO surface runoff [mm],

DP deep percolation [mm],

CR capillary rise [mm],

ΔSF change subsurface flow [mm],

ΔSW change is soil water content [mm].

The water balance equation must always equal zero to satisfy conservation of mass laws. So when all but one parameter is known, calculating the missing parameter is a simple matter. However, due to the extremely small fluxes associated with the variables over small time scales (< 1 day), accurate estimation of the unknown variables requires longer measurement intervals in the range of seven to ten days (Allen et al, 1998).

Evapotranspiration equations

Evaporation and transpiration were calculated in the study by three means. One approach for measurement of actual *ET* was accomplished by rearranging the water balance equation (Eq.1) to solve for *ET*. Two *ET* estimation methods, the FAO (Food and Agricultural Organization of the UN) Penman-Monteith and Hargreaves methods, were used in the study as well. Both estimation methods require some form of meteorological data and are formulated to provide *ET* for a grass reference surface.

Utilizing the water balance equation (Eq.1), several simplifications could be made to the formula due to the nature of the greenroof system. First, no irrigation (I) was applied due the hearty, drought tolerant vegetation. Soil moisture content, having never reached saturated during the study period (January-August, 2005), indicated that surface runoff (RO) from Eq. 3 was nonexistent most likely due to high hydraulic conductivity evident in engineered greenroof soil. Capillary rise (CR) was impossible as there is no accessible water table in the modular greenroof containers, and subsurface flow (ΔSF) was considered zero (again due to soil column containment). Finally, deep percolation (DP) was considered to be the flow leaving the drains in the aluminum green roof blocks. Once the quantity DP exits the blocks' drains, it is conveyed in the conventional manner to roof drains and then to a municipal stormwater system. Since DP in this case becomes roof surface runoff upon exiting the green roof blocks, it is hence referred to as roof runoff (RR). Accounting for this alteration and removing unused variables, the soil water balance simplifies to:

$$ET = P - RR \pm \Delta SW \tag{4}$$

The variables, precipitation (P) and change is soil water content (ΔSW), were measured directly at the study site using automated sampling equipment. Roof runoff (RR), previously called deep percolation, was measured concurrently at an adjacent site in a parallel ongoing study (Prowell, pers comm.). From this simple water balance, ET could easily be computed. As mention earlier, due to the difficulty measuring small changes in runoff and soil water content, longer intervals (7+ days) are required to obtain accurate evapotranspiration values using Eq. 4 (Allen et al, 1998).

Estimation methods such as the FAO method based on the Penman-Monteith combination equation use standard meteorological data to determine *ET* for a theoretical reference surface. The format of the equation allows calculations of *ET* on short intervals. In the current study, *ET* was calculated using this method on hourly intervals that were summed to daily totals. The Penman-Monteith combination equation relies on the necessity for any surface to obey conservation of energy laws. For the following surface energy balance based on an hourly time scale, the surface is assumed to be of zero thickness and thus mass-less and is therefore, incapable of energy storage:

$$R_n - G - \lambda ET - H = 0 \tag{5}$$

where R_n net radiation [MJ m^{-2} h^{-1}],

G soil heat flux,

λET latent heat flux,

H sensible heat flux.

Using measured radiation and soil heat flux values in the energy balance, the Penman-Monteith combination equation estimates hourly λET using the following equation:

$$\lambda ET = \frac{\Delta\left(R_n - G\right) + \rho C_p \dfrac{\left(e_s - e_a\right)}{r_a}}{\Delta + \gamma\left(1 + \dfrac{r_s}{r_a}\right)} \tag{6}$$

where λET latent heat flux [MJ m^{-2} h^{-1}],

R_n net radiation at crop surface [MJ m^{-2} h^{-1}],

G soil heat flux density [MJ m^{-2} h^{-1}],

Δ slope of the saturation vapor pressure curve [kPa $^{\circ}C^{-1}$],

γ psychrometric constant [kPa $^{\circ}C^{-1}$],

C_p specific heat of air [MJ kg^{-1} $^{\circ}C^{-1}$],

e_s saturation vapor pressure [kPa],

e_a actual vapor pressure [kPa],

$e_s - e_a$ saturation vapor pressure deficit [kPa],

r_s bulk surface resistance [s m^{-1}],

r_a bulk aerodynamic resistance [s m^{-1}].

In order to predict evapotranspiration from a plant and surface, FAO Penman-Monteith method computes evapotranspiration for a reference surface, called ET_O, using standard meteorological data along with R_n and G. As defined by the FAO Expert Consultation on Revision of the FAO Methodologies for Crop Water Requirements, the reference surface is:

> "A hypothetical reference crop with an assumed crop height of 0.12 m, a fixed surface resistance of 70 s m^{-1} and an albedo of 0.23" (Allen et al, 1998).

The reference surface most closely resembles an extensive surface of well-watered, actively growing green grass of uniform height that completely shades the surface. Using the assumptions previously mentioned, the Penman-Monteith method providing hourly reference surface evapotranspiration reduces to the following equation:

$$ET_O = \frac{0.408\Delta\left(R_n - G\right) + \gamma \frac{37}{T_{hr} + 273.16} u_2 \left(e^0\left(T_{hr}\right) - e_a\right)}{\Delta + \gamma\left(1 + 0.34u_2\right)} \quad (7)$$

where ET_O is crop evapotranspiration [mm hour^{-1}], T_{hr} is the average hourly temperature [˚C], Δ is the slope of the saturation vapor pressure curve now calculated at T_{hr} [kPa ˚C^{-1}], u_2 is the average hourly wind speed measured at 2 m [m s^{-1}], and $e^0(T_{hr})$ is the saturation vapor pressure at T_{hr} [kPa]. All other variables correspond to those in the general Penman-Monteith equation.

In order to determine the evapotranspiration for a specific crop, ET_C, the FAO method corrects ET_O using a known crop coefficient, K_c. However, in the current study crop evapotranspiration was not needed. Upon entering potential evapotranspiration in HYDRUS-1D, actual evapotranspiration, ET_C, is calculated based on water availability in the soil. In order to verify HYDRUS' predictions of ET_C, daily totals of hourly ET_C were compared to ET calculated based on the water balance equation (Eq.2). Once verified, the FAO Penman-Monteith method was assumed accurate and could be used for estimating reference evapotranspiration in any location with sufficient data available.

Hargreaves' method was also used in order to obtain evapotranspiration for a grass reference surface. The Hargreaves' method requires fewer weather parameter inputs, only average (T_{ave}), minimum (T_{min}), and maximum (T_{max}) temperature and extraterrestrial radiation (R_a) for ET calculations. This was desirable for use in the evaluation cities where several variables in the Penman-Monteith method were not available. The Hargreaves' equation follows:

$$ET_O = 0.023 * R_a (T_{ave} + 17.8)(T_{\max} - T_{\min})^{0.5} \quad (8)$$

ET_O calculated using study site weather data, the simpler method of Hargreaves was compared to the Penman-Monteith method using linear regression in order to assess the accuracy of the less data intensive method.

Modeling with HYDRUS

Using the combined heat and moisture transport program, HYDRUS-1D, the study system was simulated based on measured or estimated parameters. Input requirements for HYDRUS-1D included surface moisture fluxes (evapotranspiration and rainfall) and soil hydraulic properties. Following the hydraulic functions of van Genuchten (1980), soil hydraulic properties required included residual and saturated volumetric moisture content, θ_r and θ_s, pore size distribution index, n, the pore connectivity parameter, l, the inverse of air-entry value, α, and saturated hydraulic conductivity, K_s. Van Genuchten estimated the parameter, l, to be about 0.5 for a wide range of soil types. HYDRUS also offers neural network prediction function based on pedotransfer functions (PTF's) using Rosetta Lite version 1.1 (Schaap et al, 2001) for van Genuchten hydraulic parameters. Requirements for the neural network include volumetric moisture content at field capacity and permanent wilting point, sand, silt, and clay percentages, and bulk density.

HYDRUS also has a parameter estimation mode for which unknown soil parameters can be estimated based on measured quantities. Parameters estimated using HYDRUS included the inverse air-entry parameter, α, pore size distribution index, n, pore size index, n, and saturated hydraulic conductivity, K_s. These parameters were estimated based on measured values of soil moisture content.

Validating the HYDRUS model

In order to test the accuracy of the simulation, runs were performed and runoff values obtained were compared to actual runoff measured *in situ*. Validation runs used the parameter estimation function for non-measured hydraulic properties required by HYDRUS-1D including n, α, and K_s. Residual and saturated moisture content were extrapolated from the characteristic moisture curve obtained during the Tempe cell experiment. Results of validation are presented below.

Stormwater simulation in evaluation cities

Upon verifying the accuracy of the HYDRUS model, hypothetical modular block greenroof systems in seven evaluation cities were tested to assess stormwater runoff amounts. Using 2004 data from the National Climatic Data Center (NCDC, 2004) including minimum, maximum, and average temperature, wind speed and direction, rainfall, and others. As atmospheric boundary conditions for HYDRUS, rainfall was taken directly from published data and evapotranspiration was computed from temperature using the Hargreaves method. The evaluation cities are shown in Table 2.1. In addition to the test site greenroof system's ten cm media depth, five, fifteen and thirty cm depths were also simulated.

Results and Discussion

Laboratory soil testing

The characteristic moisture release curve obtained during the laboratory experiment is shown in Fig. 2.1. When the log of pressure head, h, was plotted against volumetric moisture content, θ, the characteristic S-shaped curve was evident with upper and lower legs approaching saturated and residual moisture content, respectively.

Table 2.1. Evaluation cities with climate type and average seasonal weather conditions

City	Climate Type	Temperature* (C)		Monthly Rainfall (cm)	
		Summer	Winter	Summer	Winter
Atlanta	moist warm-temperate	30/19	14/3	10.4	10.5
Denver	grassland (steppe)	28/12	8/-7	5.0	1.6
Honolulu	tropical	30/23	27/20	1.6	7.6
Los Angeles	summer-dry, winter wet	24/16	20/10	0.2	6.0
New York	cool-temperate	27/18	7/0	11.0	10.7
Phoenix	semidesert	39/24	21/7	1.3	1.9
Seattle	cool-temperate	22/11	9/3	3.2	13.7

Climate type adapted from Aber and Melillo, 1991.
*High/Low. Climate data from NOAA 30-yr normals for Nov-Feb and Apr-Aug

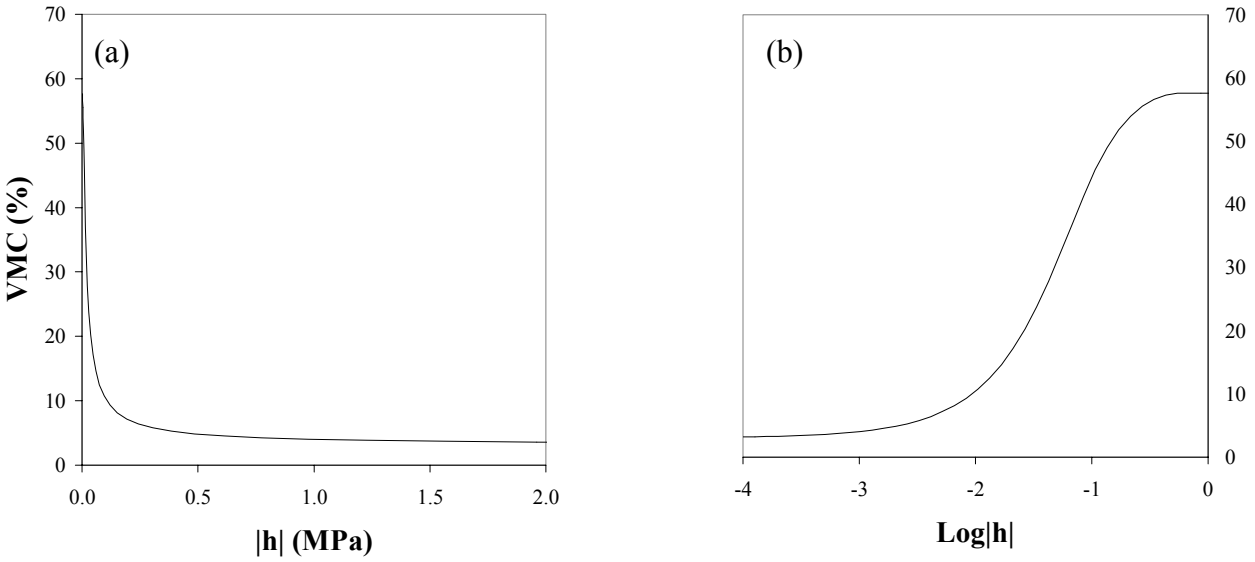

Fig. 2.1. Hydrus-simulated volumetric moisture content (%) versus (a) |h| (cm of H_2O) and (b) log |h|.

Evapotranspiration at the study site

As an input for HYDRUS-1D, an estimate for potential evapotranspiration, ET_O, was required. For the study, both the FAO Penman-Monteith and Hargreaves' methods for

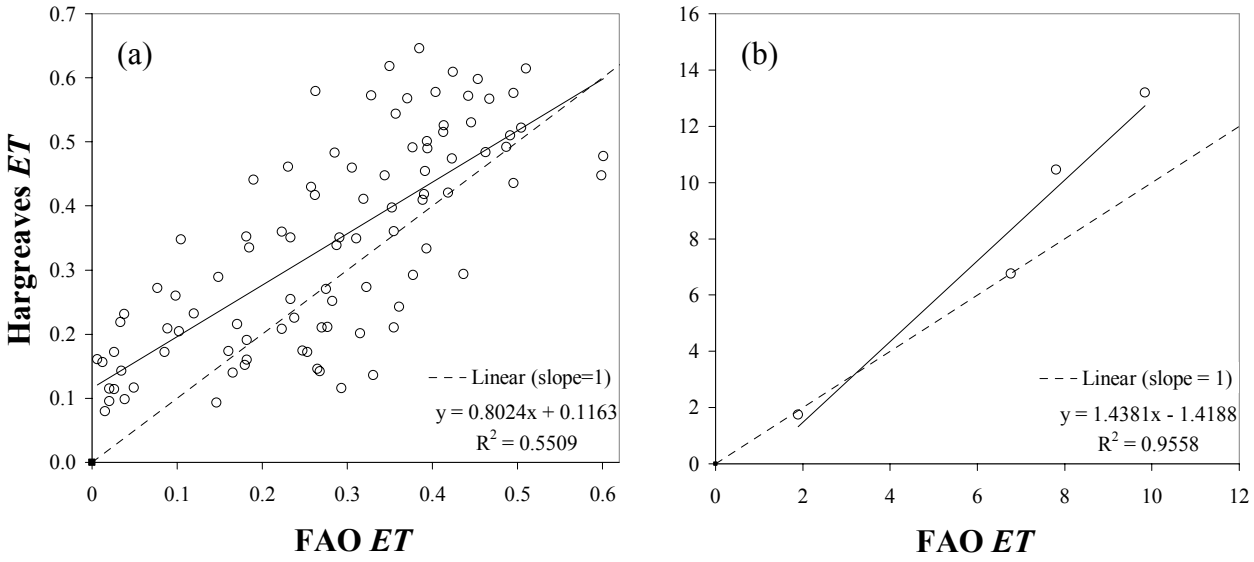

Fig. 2.2. Comparison of *ET* (cm) for (a) daily and (b) monthly weather observations.

predicting *ET* for reference crop evapotranspiration, ET_O, were used with required meteorological data collected from the greenroof study site. Data were evaluated for the period between February and July 2005, and subsequent *ET* estimations were compared by linear regression. Though the Penman-Monteith method is the most widely accepted, the evaluation has attempted to show that Hargreaves' method could be equally accurate for use in HYDRUS-1D simulations. Figs. 2.2 (a) and (b) show the results of the comparison between the FAO and the Hargreaves' methods for daily and monthly *ET* summations for the study site for the period between February and June 2005 at the study site.

Without direct inputs for solar radiation and windspeed which affect evapotranspiration, the simpler method of Hargreaves' often results in over-prediction of *ET* during periods of cloudiness, and under-prediction during times of high wind compared to *ET* predicted using the Penman-Monteith method which takes these effects into account directly. During the study period, February to June 2005, the site received higher than average rainfall meaning that higher

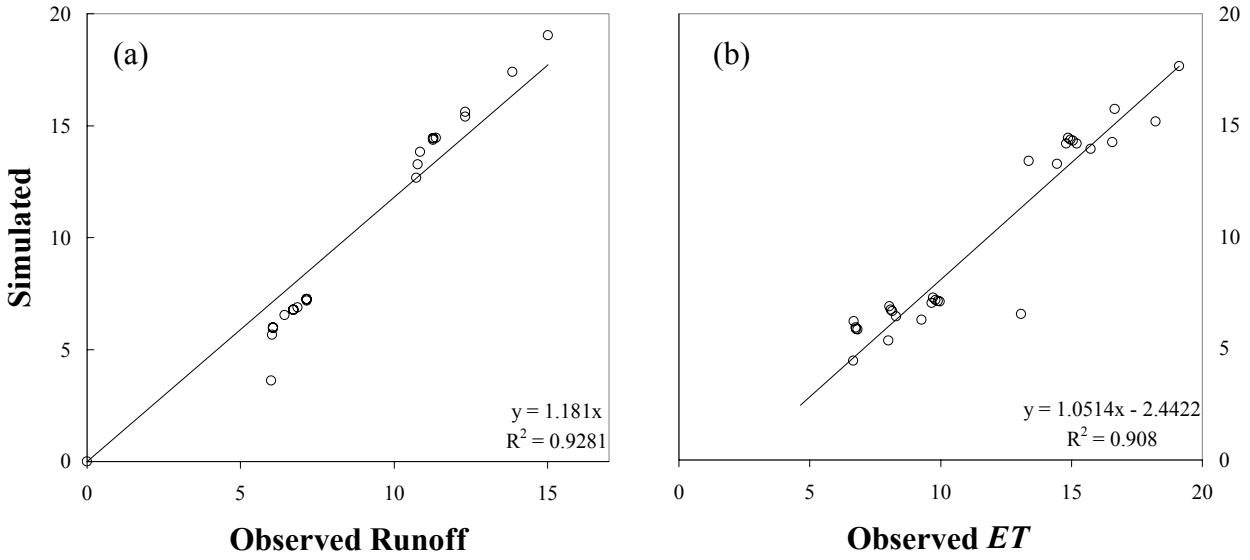

Fig. 2.3. Hydrus-simulated versus observed (a) runoff and (b) *ET*.

than average cloudiness was evident, as well. Thus, estimates for ET_O calculated using the Hargreaves' method were higher than those calculated via the Penman-Monteith method. Higher monthly ET_O predictions from Hargreaves' method are evident in Fig. 2.2 (b) since the slope of the linear correlation between Hargreaves' and the Penman-Monteith methods is 1.4. However, the relative simplicity afforded by Hargreaves' method allowed *ET* to be estimated for the seven evaluation cities of Table 2.1 for which extensive climate data required by the Penman-Monteith method were not readily available.

Simulating evapotranspiration with HYDRUS-1D at the study site

After inputting potential evapotranspiration estimates, rainfall, and soil hydraulic properties, HYDRUS-1D was used to simulate both runoff and actual evapotranspiration for the study site during June 2005. Measured runoff for June measured on site was used to verify the accuracy of the HYDRUS-derived runoff (Fig. 2.3(a)). Simulated actual evapotranspiration was validated using water balance-derived *ET* measured at the study site (Fig. 2.3(b)).

Table 2.2. Simulated runoff reduction at 5, 10, 15, and 30 cm soil depth for a 1000 m^2 roof.

City	Rainfall (m^3)	% Runoff Reduction at soil depth			
		5 (cm)	10 (cm)	15 (cm)	30 (cm)
Atlanta	1361	28%	34%	38%	43%
Denver	373	58%	70%	76%	81%
Honolulu	991	25%	29%	31%	36%
Los Angeles	511	17%	23%	27%	34%
New York	1281	31%	36%	39%	44%
Phoenix	334	35%	42%	47%	53%
Seattle	791	32%	36%	38%	42%

Stormwater in evaluation cities

Once simulated runoff values for the study site were verified using site-measured values (Fig. 2.3 (a)), runoff was simulated for the seven evaluation cities of Table 2.1. Using 2004 National Climate Data Center (NCDC) data, potential evapotranspiration was estimated using Hargreaves' method.

In addition to the soil depth used at the study site, three others, 5, 15, and 30 cm, were used to assess stormwater runoff volume. Table 2.2 shows the percent runoff reduction for a 1000 m^2 greenroof installation at each soil depth for the evaluation cities compared to an impervious roof. As evidenced by Table 2.2, significant reduction was evident for each soil depth. However, percent reduction depended strongly on the volume of rainfall per storm event as shown in Table 2.3. Cities such as Los Angeles and Phoenix that received relatively large rain event in winter when evaporative potential was low showed less runoff reduction potential than summer-wet locations. Denver, where rainfall per event was low and evaporative potential high, showed the greatest runoff reduction potential.

Table 2.3. Yearly runoff reduction as affected by rainfall per event for a 10 cm depth greenroof.

City	Season*	# of storms	Rainfall per event (cm)	Avg Daily Potential ET (mm)	Runoff Reduction (%)
Atlanta	S	32	2.5	4.5	34
	W	30	1.8	2.0	
Denver	S	27	1.2	4.8	70
	W	19	0.3	1.6	
Honolulu	S	30	0.6	4.3	29
	W	33	2.5	3.0	
Los Angeles	S	2	0.1	4.3	23
	W	17	2.9	2.2	
New York	S	37	2.2	3.8	36
	W	30	1.6	1.1	
Phoenix	S	8	0.6	6.3	42
	W	12	2.6	2.7	
Seattle	S	19	1.1	3.6	36
	W	30	1.6	0.9	

*S=summer (Apr-Sep), W=winter (Oct-Mar)

Conclusions

As stormwater concerns in urban settings have become ubiquitous, greenroofs have been introduced as a viable and effective method for reducing urban stormwater runoff from roof surfaces. The adverse impacts of stormwater surge have been widely studied, so finding methods to lessen surge is imperative. The current study successfully predicted runoff using a packaged one-dimensional moisture transport program, namely HYDRUS-1D, a reliable method for predicting stormwater runoff for a modular block greenroof system. Greenroof soil

hydraulics were measured in a laboratory setting and entered in HYDRUS along with measured rainfall and estimated potential evapotranspiration based on 2004 National Climate Data Center data.

The study concluded that modular block greenroofs reduce stormwater runoff substantially at all soil depths simulated. The analysis also showed that the ability of the greenroofs to reduce stormwater strongly depends on the amount of rainfall per storm event as well as the evaporation potential of atmosphere at each evaluation site. With increasing rainfall per event, the ability of the greenroof to reduce stormwater decreased greatly. This effect was quite obvious for cities such as Los Angeles, where large rainfall events (average, 2.7 cm) especially in winter when evaporative potential was lowest, results in smaller stormwater runoff reduction compared to an impervious roof (17-34 %). Alternately, in cities such as Denver where the majority of rainfall events occurred in summer when evaporative potential was high, runoff reduction was relatively high at 70 % for a 10 cm depth greenroof.

Increasing the soil depth of the modular greenroof blocks resulted in greater runoff potential. In Atlanta, for example, increasing soil depth from five to thirty centimeters resulted in an increase in runoff reduction from 28 % to 43 %. However, the cost of a thirty-centimeter greenroof is substantially higher. Whether or not the stormwater runoff reduction benefits outweigh the costs of increasing the soil depth of the greenroof system exceeds the scope of the research. Such an analysis depends on local laws and ordinances regarding stormwater taxes and fees for a given greenroof site.

Concerning the ability of greenroofs to reduce urban stormwater runoff, greenroof simulations have shown that potential for reduction was greatest in cities that experience the majority of rainfall during times of high evaporative potential, usually in warmer summer

months. In addition, since rainfall event size inversely affects runoff reduction potential, cities that experience smaller rain events, not necessarily fewer, are best candidates for greenroof applications.

CHAPTER 3

THERMAL CONDUCTIVITY OF AN ENGINEERED GREENROOF SOIL[2]

[2] Hilten, R. N., T. M. Lawrence, and E. W. Tollner. To be submitted to the *International Journal of Heat and Mass Transfer.*

Abstract

A method was developed to predict the thermal conductivity of an engineered greenroof soil in multiple climates. Since thermal conductivity strongly depends on soil moisture content, HYDRUS-1D, a one-dimensional moisture transport simulation was utilized to predict soil moisture based on micrometeorological data. Accuracy of simulated soil volumetric moisture was verified via a water balance model using measured parameters at a modular block greenroof system sited on the University of Georgia's Athens campus. Several models were then used to predict the thermal conductivity of the soil based on the theory of heat and moisture transfer of Philip and De Vries (1957). Thermal conductivity models included those developed by De Vries (1966), Vershinin (1966), and Campbell (1985). Accuracy of modeled thermal conductivity was assessed via comparison to data gathered from the study site. This was accomplished by comparing modeled values to an assumed steady-state thermal conductivity during early morning estimated using Fourier's heat conduction while the soil temperature gradient remained linear. Modeled values were within 10 % of actual values for the majority of observations. With accuracy verified, thermal conductivity values were then estimate for seven evaluation cities in the United States to determine the effective thermal resistance per unit area (R-value) that can be expected for a greenroof in each city.

Keywords: thermal conductivity, R-value, greenroof, engineered soil, heat transfer

Introduction

In the U.S., the green roofing industry is rapidly burgeoning, as is the concurrent need for practical information on the effects imposed by green roofing. More specifically, there is need to understand the thermal properties of greenroofs. Often thermal properties are site specific, meaning that greenroofs will often perform quite differently depending on the climate of the site. While many studies have assessed the site specific thermal properties of green roofs in various climates ranging from Mediterranean (Del Barrio, 1998; Niachou, 2001; and Theodosiou, 2003) to tropical (Wong et al, 2003), to cool temperate (Liu, 2002), no studies were found that attempted to predict thermal properties in areas other than that of the study site.

Therefore, predictive models are required to evaluate various parameters related to the ability of greenroofs to transport thermal energy. The current study introduces a method to predict the thermal conductivity of an engineered greenroof soil in multiple climates. To do so, several methods were used to calculate the thermal conductivity of the greenroof soil media. These were either based on physical characteristics of the soil (De Vries, 1966; Vershinin, 1966; Campbell, 1985) or on actual thermal parameter readings taken *in situ*. Seven U.S. cities were used for calculating thermal conductivity that represent various climate types. Table 3.1 shows evaluation cities along with their respective climate type and average seasonal weather.

Materials and methods

Calculating soil thermal conductivity

Calculating thermal conductivity models based on the physical properties generally required volumetric fractions of solid, liquid and air, which were used to estimate the soil's volumetric heat capacity. Knowing each soil fraction's individual specific heat, volumetric heat capacity was calculated for each component as specific heat multiplied by density of the

Table 3.1. Evaluation cities with climate type and average seasonal weather conditions

City	Climate Type	Temperature* (C)		Monthly Rainfall (cm)	
		Summer	Winter	Summer	Winter
Atlanta	moist warm-temperate	30/19	14/3	10.4	10.5
Denver	grassland (steppe)	28/12	8/-7	5.0	1.6
Honolulu	tropical	30/23	27/20	1.6	7.6
Los Angeles	summer-dry, winter wet	24/16	20/10	0.2	6.0
New York	cool-temperate	27/18	7/0	11.0	10.7
Phoenix	semidesert	39/24	21/7	1.3	1.9
Seattle	cool-temperate	22/11	9/3	3.2	13.7

Climate type adapted from Aber and Melillo, 1991.
*High/Low. Climate data from NOAA 30-yr normals

constituent. The linear combination of each individual volumetric heat capacity yielded the soil's overall heat capacity, C_s, using the theory developed by De Vries (1966):

$$C_s = C_m x_m + C_w \theta + C_a x_a + C_o x_o \quad (1)$$

where, C is heat capacity [J m^{-3} K^{-1}], x is volumetric fraction [m^3 m^{-3}] and subscripts m, w, a, and o represent mineral, water, air, and organic matter, respectively. For greater accuracy, the mineral fraction was separated into quartz, organic matter, clay and "other mineral" fractions. The liquid phase was assumed to be water, and the air phase was neglected due to air's low density, and hence, its low volumetric heat capacity compared the other fractions.

Once volumetric heat capacity was calculated, thermal conductivity was found via De Vries' method based on the theory of thermal conductivity of granular materials. Certain variables in the current research were given different symbols from De Vries original

formulation in order to maintain continuity. Calculating thermal conductivity of an ellipsoidal soil particle by this method required an estimate of the soil particle's shape factor, g_a, following the formula:

$$g_a = \frac{1}{2} abc \int_0^{\infty} \frac{du}{(a^2+u)^{\frac{3}{2}}(b^2+u)^{\frac{1}{2}}(c^2+u)^{\frac{1}{2}}} \tag{2}$$

where a, b, and c are the ellipsoid's axes each with a specific shape factor, g_a, g_b, or g_c. The combination of shape factors is unity:

$$g_a + g_b + g_c = 1 \tag{3}$$

The granule's a-axis was in the direction of the average temperature gradient, T_i, as defined by:

$$T_i = \frac{1}{3} \sum_{a,b,c} \left[1 + \left(\frac{k_i}{k_0} - 1 \right) g_a \right]^{-1} \tag{4}$$

where k_0, was the thermal conductivity of the continuous medium, assumed to be water. For the green roof soil, particles were assumed spherical meaning for shape factors were equal:

$$g_a = g_b = g_c = \frac{1}{3} \tag{5}$$

Finally, the formula used for calculating the overall thermal conductivity, k, of a granular material was (De Vries, 1966):

$$k = \frac{\sum_{i=0}^{N} T_i x_i k_i}{\sum_{i=0}^{N} T_i x_i} \tag{6}$$

where N is the number of types of granules, each type with different temperature gradient, T_i volumetric fraction, x_i, or individual thermal conductivity, k_i.

Heat conduction in moist porous materials also occurs due to moisture movement driven by temperature gradients (Philip and De Vries, 1957). In theory, two differential equations, one for temperature and one for soil moisture content, are needed to describe a system with heat transfer and moisture movement due to temperature gradients. Luckily, the De Vries method incorporates a simple formulation introduced by Krischer and Rohnalter (1940) to ascertain an apparent thermal conductivity to account for the influence moisture movement for soils under natural conditions. Apparent thermal conductivity, $k_{apparent}$, was defined as the sum of normal heat conductivity, k_a, and conductivity due to vapor movement, k_v, where:

$$k_{apparent} = k_a + k_v \tag{7}$$

$$k_{v^s} = \frac{LDP}{R\Theta(P - p_{w^s})} \frac{dp_{w^s}}{d\Theta} \tag{8}$$

$$D = \left(\frac{17.6}{P}\right)\left(\frac{\Theta}{273.16}\right)^{2.3} \tag{9}$$

where L latent heat of vaporization for water

D diffusion coefficient of water vapor in air

P atmospheric pressure

R gas constant for water vapor

p_w^s saturation vapor pressure

Θ virtual temperature [˚C]

Krischer and Rohnalter used the subscript v^s to designate vapor's contribution to thermal conductivity in the case where the air within soil pores is saturated. Once saturated thermal conductivity was known, unsaturated conductivity was calculated via Philip and De Vries (1957) as a function of soil humidity, h:

$$k_v = hk_{v^s} \tag{10}$$

Other formulations used for determining thermal conductivity (Vershinin, 1966, McInnes, 1981, Campbell, 1985) were based on empirical correlations and curve fitting. Campbell (1985) proposed that:

$$k = A + B - (A - D)e^{\left[-(C\theta)^E\right]} \tag{11}$$

$$A = \frac{0.57 + 1.73x_q + 0.93x_m}{1 - 0.74x_q - 0.49x_m} - 2.8x_s\left(1 - x_s\right) \tag{12}$$

$$B = 2.8 x_s \theta \tag{13}$$

$$C = 1 + 2.6 m_c^{-\frac{1}{2}} \tag{14}$$

$$D = 4 \tag{15}$$

using Eq. 11 that was formulated by McInnes (1981) using curve-fitting.

The final method used is based on Vershinin (1966) who devised an empirical model describing thermal conductivity, k, for a range of soil moisture, θ. From Vershinin (1966), it follows that:

$$k(\theta) x 10^7 = \left[2.1 \frac{\rho}{1000} (1.2 - 2\theta) e^{-0.7(\theta - 0.2)^2} + \left(\frac{\rho}{1000} \right)^{(0.8+2\theta)} \right] \rho C_s \tag{16}$$

where ρ is the soil's apparent density (kg m^{-3}) and C_s is soil volumetric heat capacity (J m^{-3}). Vershinin calculated soil volumetric heat capacity as in De Vries (1966). Del Barrio (1998) states that Vershinin's model predicts thermal conductivity for a large sample of soils with apparent density between 1100 and 1500 kg m^{-3} with relative error generally less than 7 %.

Verifying thermal conductivity

In order to verify the thermal conductivity as estimated by the de Vries (1966), McInnes (1985), and Vershinin (1966) methods, actual thermal conductivity was measured at the greenroof study site using field measurements of soil temperature and heat flux. A time, 6 am, was chosen at which point the temperature gradient was linear and solar heat flux was essentially zero. Solving Fourier's law of heat conduction for conductivity, k, assuming steady state heat transfer:

$$G = k\frac{T_s - T_{z_i}}{z_i} \tag{17}$$

where G was ground heat flux (W m^{-2}) , T_s was surface temperature (K), $T_{z,i}$ was the temperature at depth, z_i (m).

Soil moisture simulation using HYDRUS-1D

For each thermal conductivity computation method, soil volumetric moisture content, θ, is a key input parameter. In order to predict the temporal variation in θ for the engineered soil, a one-dimensional combined heat, moisture and multiple solute transport simulation, HYDRUS-1D, was used. HYDRUS-1D is actually a software package containing HYDRUS (v.7.0) along with HYDRUS-1D, a graphics-based user interface. Using the Richards' equation for variably-saturated water and convection-dispersion type equations, HYDRUS 7.0 numerically solves heat and moisture transport for a given soil (Šimůnek et al, 1998).

HYDRUS-1D requires several soil-specific and variable boundary condition parameters to simulate soil moisture fluxes in porous media. Input requirements for HYDRUS-1D included surface moisture fluxes (evapotranspiration and rainfall) and soil hydraulic properties. Evapotranspiration was calculated following Hargreaves' method (1985) using TMY (Typical Meteorological Year) data. According to Hargreaves (1985), evapotranspiration, ET_O, can be calculated by:

$$ET_O = 0.023 * R_a(T_{ave} + 17.8)(T_{\max} - T_{\min})^{0.5} \tag{18}$$

where T_{ave}, T_{min}, and T_{max} are the average, minimum, and maximum air temperatures (˚C) measured during the observation interval. R_a in Eq. 16 is extraterrestrial radiation (mm).

Hydraulic property inputs depend on the hydraulic model selected in HYDRUS-1D. With van Genuchten's (1980) hydraulic model chosen, HYDRUS requires soil hydraulic properties including residual and saturated volumetric moisture content, θ_r and θ_s, pore size distribution index, n, the pore connectivity parameter, l, the inverse of air-entry value, α, and saturated hydraulic conductivity, K_s. Van Genuchten (1980) estimates the parameter, l, to be about 0.5 for a wide range of soil types. HYDRUS also offers a neural network prediction function for these parameters. Requirements for the neural network include volumetric moisture content at field capacity and permanent wilting point, sand, silt, and clay percentages, and bulk density.

HYDRUS also has a parameter estimation mode for which unknown soil parameters can be estimated based on measured quantities. Parameters estimated using HYDRUS included the inverse air-entry parameter, α, pore size distribution index, n, pore size index, n, and saturated hydraulic conductivity, K_s. These parameters were estimated based on site-measured values of soil moisture content.

HYDRUS-1D validation

In order to verify simulated soil moisture content, HYDRUS' soil parameters were adjusted until an acceptable correlation was obtained for simulated versus observed volumetric moisture content based on linear regression analysis. Once verified, soil moisture was estimated for each of the seven evaluation cities for a greenroof system with engineered soil depth at 10 cm.

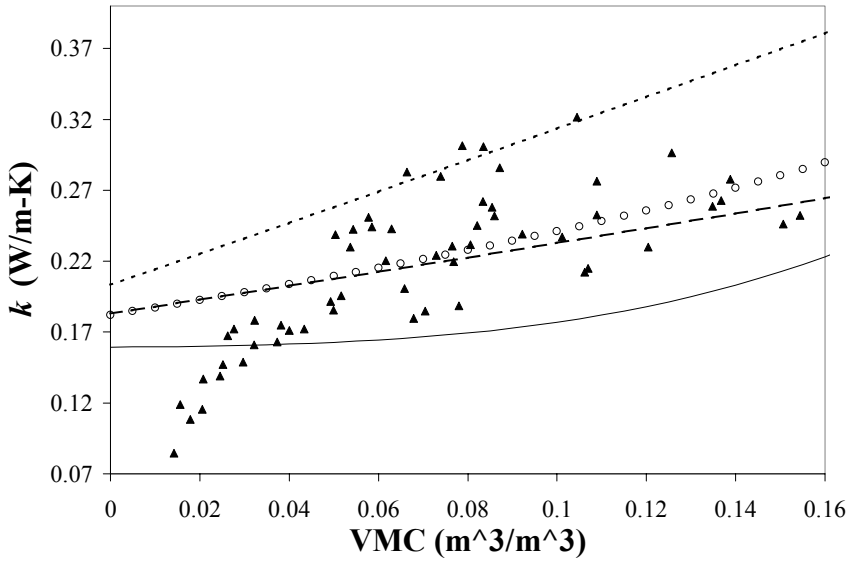

Fig. 3.1. Thermal conductivity as a function of volumetric moisture content for the various methods.

Results and Discussion

Thermal conductivity

Based on the physical properties of an engineered greenroof soil, thermal conductivity was calculated by three methods. A fourth method, based on Fourier's heat conduction equation, was assumed to be the actual measured thermal conductivity. Figure 3.1 shows the variation of soil thermal conductivity with volumetric moisture content for each of the three empirical methods, Vershinin (short dash), De Vries (long dash), and Campbell (solid line) along with actual conductivity (solid triangles). Actual conductivity was calculated at 6 am each morning at which time, the temperature profile in the soil was linear. Where actual *k* diverges from predicted *k*, measured VMC was at the extreme low end of the normal range. At such low VMC values (below 3 %), measurement error was likely due monitoring equipment limitations.

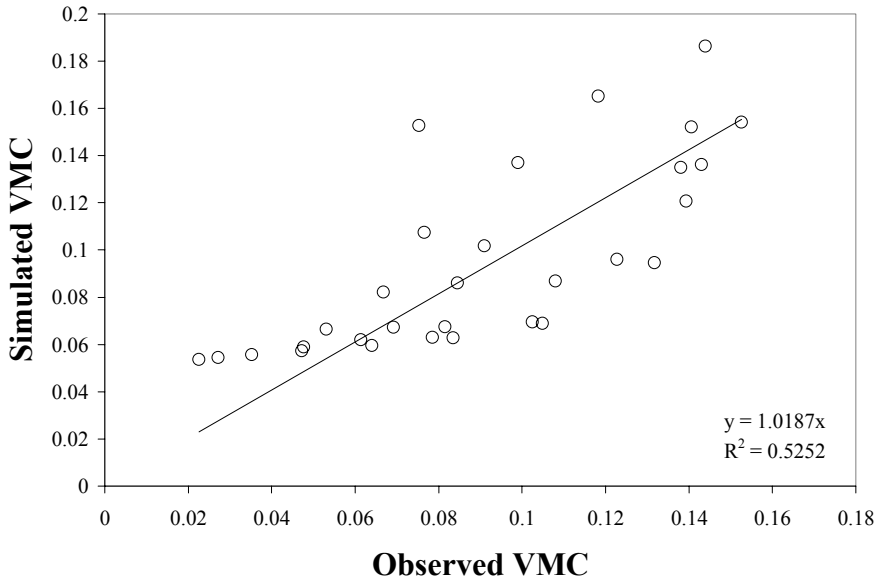

Fig. 3.2. Hydrus-simulated versus observed volumetric moisture content for April 2005.

Simulated soil volumetric moisture content validation

In HYDRUS-1D, hourly rainfall and evapotranspiration data evaluated for a representative summer and winter month (February and June, 2005) at the study site were used to simulate soil volumetric moisture content. Fig. 3.2 shows the results of the linear regression of simulated and measured soil moisture content. For the purposes of the current study, simulated VMC exhibited acceptable accuracy compared to measured moisture content. The prior assumption was made given that the error between measurements was generally less than 10 % as shown in Fig. 3.3 (with 10 % error bars) where thermal conductivity was calculated as the average of De Vries, Vershinin, and Campbell's methods for simulated and observed moisture content. An ANOVA test revealed the probability of equal variance between simulated and observed thermal conductivity was 0.8. Since the variation in thermal conductivity was low based on simulated and observed moisture content, HYDRUS simulated values were assumed acceptably accurate.

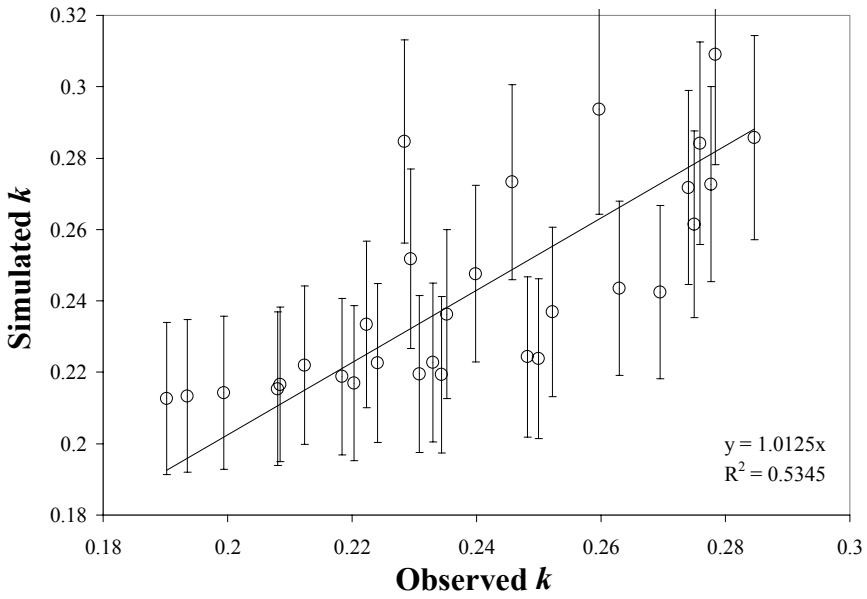

Fig. 3.3. Thermal conductivity calculated for simulated and observed VMC.

Soil moisture and thermal conductivity in evaluation cities

Once the HYDRUS simulation was validated for accuracy, rainfall and evapotranspiration estimated from TMY (Typical Meteorological Year) data available from the National Climate Data Center were entered for each of evaluation cities along with hydraulic properties for a hypothetical 10 cm soil depth greenroof sited in each city. Evapotranspiration was calculated using Hargreaves' method based on daily temperature and extraterrestrial radiation. Table 3.2 shows simulated volumetric moisture content values for each city for winter and summer months.

Using simulated VMC, an average thermal conductivity was calculated for each evaluation city for a summer and winter month. Table 3.2 shows thermal conductivity and R-value that can be expected for a 10 cm soil depth greenroof of the type used in the current study. Obvious from Table 3.2 and thermal conductivity formulation, cities that exhibited higher soil moisture content also exhibited higher R-values. Referring to Table 3.1, seasonal soil moisture

Table 3.2. Simulation results for volumetric moisture content and thermal conductivity for a 10 cm soil depth greenroof system.

City	VMC		Thermal Conductivity (W/m-˚C)		R-value (˚C-m^2/W)
	summer	winter	summer	winter	yearly
Atlanta	0.09	0.10	0.24	0.24	0.41
Denver	0.07	0.06	0.23	0.22	0.45
Honolulu	0.06	0.08	0.22	0.23	0.45
Los Angeles	0.05	0.08	0.21	0.23	0.45
New York	0.09	0.10	0.24	0.24	0.41
Phoenix	0.05	0.07	0.21	0.23	0.46
Seattle	0.07	0.11	0.23	0.26	0.41

closely mimics seasonal rainfall. For example, Seattle's winter rainfall (13.7 cm) was higher than any other evaluation city, so it was expected that volumetric moisture content would be relatively higher, which was indeed the case. The R-value exhibited by the greenroof's engineered soil was very similar to that of preformed cellular glass (R-value = 0.49 C-m^2 W^{-1}, 25 mm thickness), roof insulation common for use above roof decks (ASHRAE, 2001).

Conclusions

A model was developed to assess the thermal conductivity of an engineered greenroof soil as a function of soil volumetric moisture content for seven evaluation cities in the U.S. Thermal conductivity was calculated using three estimation methods including those of De Vries (1966), Vershinin (1966), and Campbell (1985), first for the study site and then for the evaluation cities upon validation of the estimates. Validation was accomplished by comparing thermal conductivity yielded by the estimation methods to values calculated using Fourier's

steady-state heat conduction equation. Moisture content was simulated using HYDRUS-1D and validated with moisture content measured at a greenroof site at the University of Georgia.

Soil thermal conductivity was shown to vary little for the small range of soil moisture content (average, 0.05-0.11 VMC) evident from HYDRUS simulations for the evaluation cities. Average seasonal thermal conductivity ranged from 0.21 (Los Angeles and Phoenix, summer) to 0.26 W m^{-1} $^{\circ}$C (Seattle, winter).

The study revealed that greenroofs with engineered soils provide moderate level of insulation comparable to that of preformed cellular glass (25 mm), which can also be used above roof decks. However, one shortcoming of the thermal conductivity calculation arose due the methods' inability to take into account the effects of evapotranspiration from the surface.

CHAPTER 4

MODELING ENERGY LOAD EFFECTS ASSOCIATED WITH GREENROOFING[3]

[3] Hilten, R. N., T. M. Lawrence, and E. W. Tollner. To be submitted to *Building and the Environment*.

Abstract

As greenroofs become more prevalent in the U.S., methods are needed to predict the effects imposed by the addition of a vegetated layer to a building envelope. The current study proposes a method to predict building energy loads for an extensive modular block greenroof system in multiple climates. The method incorporates two separate simulations, HYDRUS-1D and eQuest, for modeling soil moisture transfer and building energy loads, respectively. A Tempe cell experiment was conducted to assess the soil hydraulic properties of the engineered greenroof soil for use in hydraulic modeling. Input to HYDRUS-1D along with estimates for moisture fluxes, rainfall and evapotranspiration, soil moisture was simulated for each of seven evaluation cities representing various climate types of the U.S. eQuest inputs including thermal conductivity, volumetric heat capacity and surface absorptance were estimated using simulated and measured parameters. Thermal conductivity was estimated for the evaluation cities using three methods including those of De Vries (1966), Vershinin (1966), and Campbell (1985). Since eQuest is not capable of simulating the effects a transpiring surface directly, an effective surface absorptance was estimated by combining latent heat flux with reflected radiation in the standard Absorptance calculation. Simulated in eQuest, building energy loads for greenroofs at four soil depths, five, ten, fifteen and thirty centimeters were compared to both a reflective, "cool" roof and a conventional BUR (built-up roof) to determine percent load reduction compared to the BUR.

Keywords: greenroof, building energy, heating loads, cooling loads, engineered soil

Introduction

Greenroofing in the United States is a burgeoning industry. With the spread of greenroofing comes the need to understand and predict the thermal effects associated with adding a soil and vegetation layer to a building envelope. Several previous studies (Liu, 2002, Theodosiou, 1999, Del Barrio, 1998, Wong et al, 2003, and Niachou et al, 2001) have evaluated the thermal properties of greenroofs. Wong et al (2003) and Liu (2002) each evaluate the thermal effects of greenroofing in empirical studies of actual greenroof installations in Singapore and Toronto, Canada, respectively. Del Barrio (1998), Theodosiou (2003), and Niachou et al (2001) each develop mathematical models to describe heat transfer in greenroof applications. Model results are tested against empirical measurements from greenroof installations in the relatively dry Mediterranean climate in Greece. Each study tests the potential of greenroofing as passive cooling devices for building envelopes, with each failing to show any passive cooling. However, in a greenroof study in Singapore's moist, tropical climate, Wong et al (2003) was able to show passive cooling for a greenroof installation. Wong et al attributes the passive cooling to solar energy absorption by evapotranspiration and photosynthesis. All studies show reduced energy loads for greenroof-topped buildings in summer months.

Though previous studies have shown that greenroofs perform differently in wet, tropical (Wong et al, 2003) and Mediterranean climates (Theodosiou 2003, Del Barrio, 1998, and Niachou et al, 2001), no studies were found that explicitly predict greenroofing effects at sites other than the study site. Such prediction is necessary for greenroofing to reach the level of application in other areas, such as Europe where in Germany alone. In 2003, it was estimated that over 145,000,000 square feet of roof space were topped with greenroof (Herman, 2003). In spite of the success abroad, building designers and users in the U.S. have yet to adopt

greenroofing widely. One reason for this is that since there are so few greenroofs in the U.S., benefits realized by the greenroofing here are yet to be shown. Often, evaluation methods in the greenroof studies are too intractable and time consuming for building designers to utilize. Thus, a simple, climate-adaptive method is needed to predict the energy load effects of green roofing for diverse climate regimes.

In the current study, a new method was introduced to predict the energy load effects associated with greenroofing. As part of the method, a simulation was used in which a rooftop vegetation layer was coupled with a standard building envelope using eQuest (QUick Energy Simulation Tool), a commonly used building energy simulation driven by DOE-2 with a user-friendly graphics-based interface. eQuest requires inputs of thermal conductivity, density, heat capacity, thickness, and surface absorptance to describe a roof layer. As thermal properties were not available for the engineered greenroof soil, a method was developed to estimate them. In addition, a method was needed to include the effects of evapotranspiration in eQuest. Using weather data, characteristic thermal and hydraulic properties were assessed for a modular block greenroof system in seven evaluation cities in the U.S. representing various climate types. Thus, yearly energy loads for buildings covered with greenroofs can be estimated for any city where TMY data is available. In the present research, seven evaluation cities in the U.S. are tested using eQuest to determine energy loads for heating and cooling.

Materials and methods

The study site

The site consisted of a green roof installation on the University of Georgia's Athens campus. The green roof was of a modular block design donated to the University of Georgia by Green Roof Blocks, a subsidiary of St. Louis Metalworks Company. The blocks consisted of are

square (60 x 60 cm) aluminum containers with depth, 10 cm. The block had three 0.64-centimeter diameter holes drilled in the base of each side to allow water to drain. Blocks were filled with approximately ten centimeters of a low-density engineered soil media composed of 80 % expanded slate and 20 % organic matter (in this case, worm castings). Greenroof vegetation consisted of five species of *Sedum*, a low-lying, succulent stonecrop. *Sedum* species included spp. reflexum, sexangulare, immegrauch, spurium, and album.

Measurements

In situ measurements were obtained using an automated weather station that collected meteorological parameters including wind speed, humidity, temperature, and net and solar radiation. Additional measured variables included volumetric moisture content, soil heat flux and soil temperature. Site-measured variables were collected on fifteen-minute intervals as averages of ten-second observations using a Campbell Scientific, Inc. CR23X datalogger.

Calculating soil thermal conductivity and heat capacity

Several methods were used to calculate the thermal conductivity of the soil. These were either based on physical characteristics of the soil (De Vries, 1966, Vershinin, 1966, McInnes, 1981, Campbell, 1985) or on actual thermal parameter measurements observed *in situ*. Actual thermal conductivity was assessed using Fourier's heat conduction equation in early morning when steady-state conditions were assumed. Thermal conductivity models based on the physical properties generally required volumetric fractions of solid, liquid and air, which were used to estimate the soil's volumetric heat capacity. For a detailed analysis of thermal properties of the engineered greenroof soil, please see Hilten et al, 2005b. Avoiding intricate details, thermal conductivity was calculated as a function of soil volumetric moisture content (m^3 water per m^3 of soil). Therefore, a method to predict soil moisture was developed in the study.

Laboratory experiments

In addition to site measurements, a lab experiment was conducted to evaluate the characteristic moisture release curve for the engineered soil, from which, inputs were obtained for soil volumetric moisture content ($m^3\ m^{-3}$) simulations. Using pressurized Tempe cells, a characteristic moisture release curve was determined that describes the volumetric moisture content of a soil versus pressure. Applied pressure at 33 and 1500 kPa correspond to the soil's field capacity and wilting point moisture content, respectively. Tempe cells of known volume were packed with intact green roof soil cores, and then were fully saturated using a 0.01 M calcium chloride solution. The cells were then enclosed in a pressure chamber with a selectively permeable ceramic bottom plate. Various pressures (1, 3, 9, 19, 33, 75, and 1500 kPa) were applied to a valve on the tops of the pressure chambers. Each pressure setting was maintained until equilibrium was reached where the weight of each cell no longer fluctuated. Weight was then recorded and the next pressure setting was applied. From the weights observed, gravimetric moisture content can be calculated by:

$$w = \frac{mass_{water}}{mass_{soil,od}} \tag{1}$$

where w gravimetric water content [kg m^{-3}],

$mass_{water}$ ($mass_{soil,wet} - mass_{soil,od}$) [kg],

$mass_{soil,od}$ mass of oven-dried soil [kg].

Equation 1 was used to determine gravimetric water content at each of the prescribed pressure settings. Volumetric water content was then determined by:

$$\theta = w\frac{\rho_b}{\rho_l} \tag{2}$$

where θ volumetric water content [m^3 (water) m^{-3} (soil)],

ρ_b soil bulk density [kg m^{-3}],

ρ_l density of water [kg m^{-3}].

Again, water content was computed for each of the pressure settings but this time as a volumetric fraction. Using pressure settings versus volumetric water content, a characteristic curve for the green roof soil was then plotted. With volumetric water content plotted on a log scale on the x-axis, the characteristic s-shape curve was evident. The upper portion (lower pressure) was assumed to be approaching θ_s, the saturated water content, and the lower region (higher pressure) approaching θ_r, the residual water content, of the soil.

Simulations

For the experiment, two packaged computer simulations were used to model the greenroof system in seven evaluation cities. The first, HYDRUS-1D (Šimůnek et al, 1998), was used in order to estimate soil moisture for the desired months (January and July) based on physical measurements. Since soil moisture is a defining variable for soil thermal conductivity (De Vries, 1966, Del Barrio, 1998), an accurate estimate of soil moisture was essential. Once soil moisture could be predicted, thermal conductivity and heat capacity were evaluated.

Soil moisture simulation

For the building energy simulation, several parameters were required as inputs to define the vegetation and soil layers of the green roof system. These parameters included density, heat

capacity, absorptance, and thermal conductivity. The latter, the thermal conductivity for the soils and soils in general, is strongly dependent on soil moisture. Therefore, a method to predict soil moisture was developed for this purpose. To predict soil moisture for the seven evaluation cities, HYDRUS-1D (Šimůnek et al, 1998), a one-dimensional heat and moisture transport simulation for variably-saturated media was utilized. Based on Richards' equation for variably-saturated water flow and convection-dispersion type heat transport equations, HYDRUS-1D simulates the heat and moisture fluxes amid a soil-plant-atmospheric continuum.

Simulating with HYDRUS-1D requires the measurement of various parameters to be used as inputs. The main inputs include soil specific parameters (saturated and residual hydraulic conductivity, soil type) and several variables (soil temperature or heat flux, evapotranspiration, rainfall). Using the HYDRUS-1D parameter estimation function, both hydraulic and heat transport parameters were simulated based on user inputs. HYDRUS calculated a soil characteristic curve that was compared to curve obtained via the Tempe cell experiment to validate HYDRUS' results. Additionally, another of HYDRUS' parameter estimates, soil moisture content, was compared to actual measurements of volumetric moisture content ($m^3\ m^{-3}$) to further verify accuracy of the simulation.

Upon validation of the HYDRUS model, evapotranspiration values calculated from TMY (Typical Meteorological Year) data from seven evaluation cities shown in Table 4.1 were entered to HYDRUS during a summer and a winter month to determine volumetric soil moisture values for the engineered green roof soil. With an accurate estimate of soil moisture, soil thermal conductivity was then calculated.

Table 4.1. Evaluation cities with climate type and average seasonal weather conditions

City	Climate Type	Temperature* (C)		Monthly Rainfall (cm)	
		Summer	Winter	Summer	Winter
Atlanta	moist warm-temperate	30/19	14/3	10.4	10.5
Denver	grassland (steppe)	28/12	8/-7	5.0	1.6
Honolulu	tropical	30/23	27/20	1.6	7.6
Los Angeles	summer-dry, winter wet	24/16	20/10	0.2	6.0
New York	cool-temperate	27/18	7/0	11.0	10.7
Phoenix	semidesert	39/24	21/7	1.3	1.9
Seattle	cool-temperate	22/11	9/3	3.2	13.7

Climate type adapted from Aber and Melillo, 1991.
*High/Low. Climate data from NOAA 30-yr normals for Nov-Feb and Apr-Aug

Modeling with eQuest

In the second simulation, building energy loads were simulated using eQuest, a commonly used building energy simulation based on DOE-2 coding, using soil volumetric moisture results from HYDRUS-1D. Other than thermal conductivity and heat capacity of roof components, parameters required by eQuest for the greenroof layer included absorptance (1 – albedo).

Absorptance

A required parameter for modeling, absorptance was calculated as a yearly average for greenroof installations in each evaluation city. The absorptance of a surface describes the fraction of radiation absorbed by a surface. For all surfaces, a fraction of radiation is absorbed, reflected and transmitted. These fractions, called absorptance (α), reflectance (ρ), and transmittance (τ), add to one. Since a surface such as a greenroof is opaque, the fraction of radiation that is transmitted is zero, i.e. τ = zero, meaning that:

$$\alpha = 1 - \rho \tag{19}$$

or,

$$\alpha = 1 - \frac{\rho R_s}{R_s} \tag{20}$$

where R_s is radiation (W m^{-2}). For the greenroof surface, a baseline ρ was taken as 0.3, which is an average between light gray soil (0.35) and short grass (0.26) (Pielke, 2002). However, for modeling purposes, absorptance was calculated to include the effects of evapotranspiration (latent heat flux), as well, for which the building energy modeling, eQuest, could not otherwise account. To do so, latent heat flux was added to the reflected portion of radiation from Eq. 20, viz:

$$\alpha = 1 - \frac{\rho R_s + \lambda LE}{R_s} \tag{21}$$

where λLE is latent heat flux (W m^{-2}) calculated from actual evapotranspiration simulated using HYDRUS-1D. An average value for the adjusted absorptance was calculated for each of seven evaluation cities. For Seattle in particular, absorptance was calculated for three additional soil depths, five, fifteen, and thirty centimeters to determine the effects of soil depth on building energy loads.

Once thermal conductivity, heat capacity, and absorptance were estimated, energy load simulations were run using eQuest. For the study site city, Athens, GA, a typical office building

was designed with three different heights, 1, 3, and 8 stories, each with two different footprint shapes (both at 929 m^2 (10,000 ft^2)); one square, and one with length two times its width.

Office building design specifics

The office building designed used a metal frame roof and walls with three inches of polyurethane insulation (R-18) in roof and R-19 batt in walls. The percent area for windows floor to ceiling for all sides of building was 57 % with overall window area percentage at 40 %. Approximately 75 % of building interior space was devoted to offices and conference rooms. Offices (70 % of overall area) had defined loads at 1.3 W/sq ft for lighting, 0.4 W/sq ft for task lighting and 1.5 W/sq ft for plug loads. The building was defined as occupied during normal business hours (8 am to 5 pm). The HVAC system consisted of chilled water coils for cooling (setpoint at 76 ˚F) and hot water coils for heating (setpoint at 70 ˚F) with a drybulb economizer. Heating was supplied by natural gas.

Roof design

The baseline roof design materials (inside to outside) consisted of roof construction mat (R-2.8), 5/8-inch plywood, 3 inches of polyurethane insulation, and an exterior gravel-covered 3/8-inch BUR (Built-Up Roof). The standard BUR specifications were an absorptance of 0.6, and a surface roughness of 1. Calculated U-value for the baseline roof design was 0.043 [Btu/h-ft^2-˚F]. To the BUR layer, four different roof coverings, a greenroof and two reflective, "cool" roofs (α = 0.1, 0.4), were simulated and compared to the standard, gravel covered BUR. In all, twenty-four building design combinations were run for the Athens, GA site. Cool roofs at α = 0.1 and 0.4 were simulated to show the broadest range of values available from manufacturers. The greenroof layer for the Athens simulation consisted of a four-inch layer of engineered soil

above a ¼ inch air layer beneath the modular blocks. The calculated U-value for this roof type was 0.035 Btu $h^{-1}ft^{-2}$ $°F^{-1}$.

In all the evaluation cities of Table 1, yearly energy loads for four roofs were simulated. Roofs included a cool roof (α = 0.15), representative of many common cool roofs currently offered, a greenroof with absorptance varying with latent heat flux, and two BUR's (α = 0.64, 0.91) representing a smooth black and a gravel-covered BUR. Additionally for Seattle, WA, three alternate soil depths, five, fifteen and thirty centimeters were simulated in addition to the study site ten-centimeter greenroof.

Results and Discussion

Laboratory experiment

The physical testing of the green roof soil resulted in a characteristic moisture release curve (Fig. 4.1) with volumetric moisture content plotted as a function of the log of pressure head. The experiment tested seven pressure heads corresponding to 1, 3, 9, 19, 33, 75, and 1500 kPa. To reiterate, due to nature of the testing procedure, pressure head as opposed tension head was tested. Water content was assumed to be equivalent in tension and compression. From the experiment, results revealed that at field capacity and wilting point, volumetric moisture content for the engineered greenroof soil was approximately 18 % and 8.2 %, respectively. These results were used for HYDRUS-1D simulations to obtain both soil moisture and actual evapotranspiration.

Soil thermal conductivity

Using the estimation methods introduced by De Vries (1966), Vershinin (1966), and Campbell (1985), the variation of thermal conductivity with soil moisture was determined for the engineered greenroof soil. Fig. 4.1 shows this relationship as compared to the actual

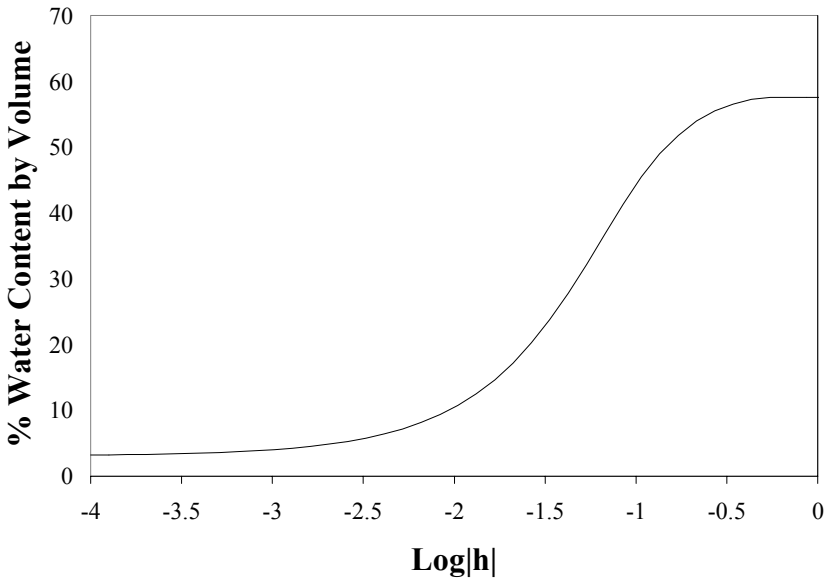

Fig. 4.1. Soil characteristic moisture release curve simulated in HYDRUS-1D.

conductivity calculated using Fourier's heat conduction equation. An average was taken of the three methods was used to determine the thermal conductivity expected in each of the evaluation cities based on HYDRUS-simulated soil volumetric moisture content.

Surface absorptance

For each of the seven evaluation cities of Table 4.1, a surface absorptance was found by combining the effects of evapotranspiration with those of radiation using Eq. 21. Evapotranspiration was simulated in HYDRUS-1D with inputs of soil hydraulic properties, potential evapotranspiration, and rainfall. Daily evapotranspiration was found using Hargreaves' method (1985) based on daily temperatures and extraterrestrial radiation estimates. Table 4.2 shows the results of the absorptance analysis.

In all cases, the effective absorptance was lowered compared to a baseline condition of α = 0.7 (estimate from Pielke, 2002) that did not include the effects of evapotranspiration. In cities

Table 4.2. Surface characteristics calculated for greenroof using Eq. 21 based on evapotranspiration.

City	Surface Characteristics			
	Cool roof		Green roof	
	reflectivity	absorptivity	reflectivity	absorptivity
Atlanta	0.85	0.15	0.54	0.46
Denver	0.85	0.15	0.42	0.58
Honolulu	0.85	0.15	0.44	0.56
Los Angeles	0.85	0.15	0.38	0.62
New York	0.85	0.15	0.61	0.39
Phoenix	0.85	0.15	0.33	0.67
Seattle	0.85	0.15	0.64	0.36

where soil moisture available for evapotranspiration was plentiful, such as Seattle, Atlanta, and New York, actual evapotranspiration transported a significant amount of latent heat from the surface. For such cities, effective α was reduced by more than 50 % with α in the range 0.36-0.46. Conversely, in cities with little rainfall such as Denver, Phoenix and Los Angeles, little soil moisture was available for evapotranspiration. Lower evapotranspiration in these cities translated to a higher effective α in the range of 0.58-0.67.

eQuest results

Initial simulation runs were made using eQuest for the study site city, Athens, GA. For the Athens site, energy loads were simulated for three building heights each with two footprint shapes (at 929 m^2). The goal of simulating several building heights was to determine how percent load reductions change with additional stories and shapes. In addition on each building, four roof types including a gravel-covered BUR, two cool roofs, and an extensive green roof were simulated. Results of cooling load simulations for Athens are shown in Table 4.3. Cooling

Table 4.3. Simulation results for (a) annual cooling loads (GJ), (b) cooling load reduction (GJ), and (c) cooling load reduction (%) for a building in Athens, GA.

(a)			Annual Cooling Load (GJ)		
Roof Type	Footprint Shape	Absorp-tance	1 story	3 stories	8 stories
BUR	Square	0.6	466	1412	4705
	Rectangular	0.6	481	1466	4936
White, cool roof	Square	0.1	443	1375	4588
		0.4	455	1384	4597
	Rectangular	0.1	458	1423	4800
		0.4	470	1432	4809
Greenroof	Square	0.31	451	1402	4696
	Rectangular	0.31	466	1456	4906

(b)			Cooling Load Reduction* (GJ)		
Roof Type	Footprint Shape	Absorp-tance	1 story	3 stories	8 stories
White, cool roof	Square	0.1	23.1	36.9	117.6
		0.4	11.1	28.2	108.1
	Rectangular	0.1	23.3	42.1	136.8
		0.4	11.2	33.4	127.2
Greenroof	Square	0.31	15.3	10.0	9.6
	Rectangular	0.31	15.2	9.8	30.1

(c)			Cooling Load Reduction* (%)		
Roof Type	Footprint Shape	Absorp-tance	1 story	3 stories	8 stories
White, cool roof	Square	0.1	5.0	2.6	2.5
		0.4	2.4	2.0	2.3
	Rectangular	0.1	5.0	3.0	2.9
		0.4	2.3	2.3	2.6
Greenroof	Square	0.31	3.3	0.7	0.2
	Rectangular	0.31	3.2	0.7	0.6

*load reductions calculated as compared to loads for the BUR in Table 4.3 (a).

Table 4.4. Simulation results for (a) annual heating loads (GJ), (b) heating load reduction (GJ), and (c) heating load reduction (%) for a building in Athens, GA.

(a)			Annual Heating Load (GJ)		
Roof Type	Footprint Shape	Absorp-tance	1 story	3 stories	8 stories
BUR	Square	0.6	8.5	23.9	66.0
	Rectangular	0.6	9.4	26.9	74.1
White, cool roof	Square	0.1	7.9	20.0	55.8
		0.4	7.6	19.8	55.4
	Rectangular	0.1	8.8	22.4	63.1
		0.4	8.5	22.3	62.6
Greenroof	Square	0.31	8.4	23.8	65.8
	Rectangular	0.31	9.4	26.8	74.5

(b)			Heating Load Reduction* (GJ)		
Roof Type	Footprint Shape	Absorp-tance	1 story	3 stories	8 stories
White, cool roof	Square	0.1	0.5	3.9	10.2
		0.4	0.8	4.1	10.6
	Rectangular	0.1	0.6	4.5	10.9
		0.4	0.9	4.7	11.5
Greenroof	Square	0.31	0.1	0.2	0.2
	Rectangular	0.31	0.0	0.2	-0.4

(c)			Heating Load Reduction* (%)		
Roof Type	Footprint Shape	Absorp-tance	1 story	3 stories	8 stories
White, cool roof	Square	0.1	6.3	16.5	15.4
		0.4	9.8	17.3	16.1
	Rectangular	0.1	6.8	16.8	14.8
		0.4	9.9	17.4	15.5
Greenroof	Square	0.31	0.9	0.7	0.3
	Rectangular	0.31	0.2	0.7	-0.6

*load reductions calculated as compared to loads for the BUR in Table 4.4 (a).

load reductions shown in Table 4.3 (b and c) in energy equivalent and in percent were obtained by comparing loads from the two cool roofs and the greenroofs to loads simulated for the gravel-covered BUR ($\alpha = 0.6$) as evident in Table 4.3 (a). Table 4.3 (b) shows annual cooling loads reduction as an energy equivalent (GJ) for each of the four roof types. As building height increased, the cool roof covered buildings revealed increased cooling load reduction compared to the BUR. Cooling loads were greater for rectangular buildings compared to square footprint buildings due to changes in south facing exposure. However, the percent reduction (Table 4.3 (c)) generally decreased with increasing height for the cool roof buildings. For the greenroof topped buildings, load reduction as an energy equivalent decreased with increasing height with the exception of the eight-story, rectangular building for which the load reduction was highest. For percent reduction, however, the greenroof buildings showed a consistent decrease with increasing building height.

Concurrent simulation results for heating loads for the hypothetical building sited in Athens, GA are shown in Table 4.4. Similar to cooling load reduction, heating load reduction (in GJ) from Table 4.4 (b) for the cool roofs increased with increasing building height while load reduction in percent (Table 4.4 (c)) peaked for the three-story buildings. Rectangular buildings exhibited higher heating loads than square buildings, again due to the amount of southern exposure. Simulations for the greenroof buildings exhibited similar loads to the BUR for all heights tested with percent reductions peaking close to 1 % for the one-story building.

The next group of eQuest runs simulated building energy loads for the seven evaluation cities of Table 4.1. For this group of simulations, square one-story office buildings were topped with a greenroof (α = location specific), a white roof ($\alpha = 0.15$), or one of two BURs ($\alpha = 0.64$, 0.91 for gravel-covered and smooth bitumen, respectively). Percent load reduction calculations

Fig. 4.5. Simulation results for annual heating and cooling loads (GJ) for four roof coverings.

City	Total Annual Load (GJ)							
	Smooth BUR		Gravel BUR		Cool roof		Greenroof	
	cooling	heating	cooling	heating	cooling	heating	cooling	heating
Atlanta	459	9.4	448	9.7	433	10.1	439	9.4
Denver	273	18.5	265	19.0	252	19.8	259	18.4
Honolulu	795	0.0	781	0.0	761	0.0	775	0.0
Los Angeles	322	2.0	311	2.2	297	2.6	307	2.0
New York	314	18.4	307	18.8	296	19.2	299	18.5
Phoenix	743	2.7	723	3.0	693	3.2	715	2.7
Seattle	210	18.2	204	18.5	196	19.1	195	18.3

compared the smooth BUR ($\alpha = 0.91$) to each of the other three roof types. Table 4.5 shows each evaluation city's annual heating and cooling load as simulated in eQuest.

Table 4.6, (a) and (b), shows heating and cooling load reductions for the gravel BUR, the cool roof, and the greenroof compared to the baseline smooth BUR. Load reduction as an energy equivalent (GJ) was greatest for Phoenix for both the cool roof and greenroof, though the percent reduction reached a maximum of 8 % for Denver, CO. Reductions were attributed to the decrease in surface absorptance for each roof type compared to the smooth BUR. The decrease in effective surface absorptance for the greenroofs was due to the effects of evapotranspiration calculated using Eq. 21, as discussed previously. Heating loads (Table 4.6 (b)) actually increased for the majority of buildings, despite roof covering, due to the high absorptivity of the smooth BUR that absorbed more solar radiation during cooler months, which lowered heating needs of the buildings. Reflective, cool roofs, by design, reflect as much solar radiation as possible meaning that little winter heat gain is possible. Only the greenroof showed any heating

Fig. 4.6. Yearly heating and cooling load reductions in (a) energy equivalent (GJ) and (b) percent.

(a)

City	Load Reduction* (GJ)					
	gravel BUR		white (cool) roof		greenroof	
	cooling	heating	cooling	heating	cooling	heating
Atlanta	10.7	-0.3	26.5	-0.8	20.2	0.0
Denver	8.9	-0.5	21.7	-1.3	14.9	0.1
Honolulu	13.8	0.0	33.9	0.0	19.8	0.0
Los Angeles	10.4	-0.2	24.3	-0.5	15.2	0.0
New York	7.2	-0.3	17.5	-0.8	14.8	-0.1
Phoenix	20.0	-0.2	50.2	-0.5	28.7	0.0
Seattle	5.3	-0.3	13.7	-0.9	14.5	-0.1

(b)

City	Load Reduction* (%)					
	gravel BUR		white (cool) roof		greenroof	
	cooling	heating	cooling	heating	cooling	heating
Atlanta	2.3	-3.0	5.8	-8.0	4.4	-0.5
Denver	3.3	-2.7	8.0	-7.1	5.5	0.7
Honolulu	1.7	0.0	4.3	0.0	2.5	0.0
Los Angeles	3.2	-11.0	7.6	-26.7	4.7	1.0
New York	2.3	-1.7	5.6	-4.3	4.7	-0.4
Phoenix	2.7	-7.9	6.8	-17.6	3.9	1.6
Seattle	2.5	-1.7	6.5	-5.1	6.9	-0.8

*load reductions calculated as compared to loads for the smooth BUR in Table 4.5.

load reductions, though percent reduction was small. Heating load reductions were attributed to increased insulation capabilities of the greenroof system compared to the smooth BUR.

For one evaluation city, Seattle, energy loads were simulated for three additional soil depths (5, 15, and 30 cm) in order to assess the effects of depth on heating and cooling loads.

Table 4.7. Load and cost reductions for greenroofs at four depths compared to a smooth BUR for Seattle, WA.

Soil Depth (cm)	Absorp-tivity	Load Reduction (%)		Cost Reduction ($)		
		Cooling	Heating	Cooling	Heating	Total
5	0.40	5.7	-1.3	54	-25	28
10	0.36	6.9	-0.8	64	-15	49
15	0.34	7.3	-0.4	68	-7	61
30	0.32	7.1	0.9	68	17	85

Table 4.7 shows the results of the simulation. Cooling loads reductions ranged from 5.7-7.3 % with reductions generally increasing with increased soil depth.

In addition to energy load calculations, energy cost comparisons were performed for the Seattle greenroof site, as well (Table 4.7). Total cost reduction ranged from $28 (5 cm depth) to $85 (30 cm depth) per year compared to a smooth BUR ($U = 0.043$ W m^{-2} °C^{-1}, $\alpha = 0.91$). At $160 m^{-2} for a 10 cm depth greenroof system, a 929 m^2 roof as in the simulations would total $150,000. In addition, the modular block greenroof system is generally placed on a waterproof BUR, which would cost approximately $60,000 for a total of $210,000 for the initial setup.

According to Kelly Luckett, manufacturer of the greenroof blocks, the lifespan of a typical 10 cm greenroof could exceed that of a conventional roof by 200 % (60 as opposed to 20 years). By the time the greenroof would need to be replaced at approximately 60 years, a conventional roof would be reaching its third replacement at a cost of approximately $60,000 each time (for a 929 m^2 roof). Therefore, the total cost for a conventional roof would have reached a total of $240,000 when including the initial roof cost. At the time of replacement for the greenroof system, on the other hand, total costs would reach $417,000 for the initial setup

and the replacement (including underlying BUR layer) minus the energy cost savings ($3000 over 60 years). Assuming the hypothetical building lasted an additional sixty years, the total for a conventional roof would approach $320,000 while the greenroof would reach $624,000. With this in mind, the 10 cm depth greenroof system would never pay for itself if only energy loads are included in the comparison.

As expected, deeper greenroof depths reduced costs compared to shallower depths. Heating cost reduction was assumed to be due to the enhanced insulation capabilities of the thicker soil layer due to lower overall heat transfer coefficients (U = 0.216, 0.210, 0.199, and 0.176 $W\,m^{-2}\,{}^{\circ}C^{-1}$ for depths 5, 10, 15, and 30 cm, respectively). In addition, deeper soils provided more moisture allowing more latent heat flux, which lowered the effective absorptance and cooling costs in summer months for the greenroof surface.

Summary and Conclusions

A method has been proposed to assess the effects of greenroofs on building energy loads in multiple climates. Results showed that greenroofs can provide a unique method to help reduce heating and cooling costs for insulated office buildings. Due to evapotranspiration and insulation effects, greenroofs limit heat transferring through building envelopes.

Using eQuest, building energy loads were simulated for various roof coverings including greenroofs, cool roofs, and conventional BURs. Simulations showed cooling and heating load reductions in the range of 2.5-6.9 % and –0.8-1.6 %, respectively, for a hypothetical ten-centimeter soil depth greenroof sited in seven U.S. cities. The cool roof showed cooling load reductions in the range 4.3-8.0 % while heating loads actually increased by 0-11 %. From this analysis, cool roofs perform best in locations with high solar loads in summer such as Los Angeles and Phoenix, where winters are mild. However, as percent reduction depends on the

annual load, actual heating and cooling loads reductions (from Table 4.6 (b)) estimated by an energy equivalent for each city may better describe the influence of roof type on heating and cooling loads. For example, for a city with very low heating loads such as Los Angeles, the percent load reduction for a cool roof was –27 % though the actual load reduction was only –0.5 GJ meaning that winter performance for the cool roof was much better than was evident by percent reduction alone.

The modular block greenroof systems simulated in the evaluation cities showed better performance in summer compared to a smooth BUR while winter performance was similar to the BUR. The analysis revealed that deeper soils act to insulate buildings more effectively than shallower depths, meaning that winter heating loads decreased with increasing depth.

Though cost comparisons showed that greenroofs have long payback periods in terms of saved energy costs alone, other benefits such as stormwater reduction, noise dampening, increased lifespan and urban heat island effects may outweigh the added cost. In a previous study by Hilten et al, 2005a, greenroofs were shown to reduce stormwater volume in range of 17-81 % compared to an impervious roof for the evaluation cities of the current study. In locations where taxes are levied for urban runoff, greenroofs could prove much more beneficial in terms of cost when reduced stormwater taxes are included with energy cost reductions.

CHAPTER 5

THESIS CONCLUSION

The manuscripts herein outline a comprehensive method to predict stormwater runoff and building energy loads for greenroofs in multiple climates. The study as a whole involved a field study, a laboratory study of soil hydraulic properties, and two simulation components to predict stormwater runoff and building energy loads.

Chapter Two provided methodology for simulating stormwater runoff for a greenroof using an engineered soil. HYDRUS-1D was employed for the simulations. Input parameters included volumetric moisture content at field capacity and wilting point, potential evapotranspiration, and rainfall. HYDRUS calculated remaining parameters by neural network prediction and parameter estimation coding. Field capacity and wilting point were assessed during a laboratory study of the hydraulic properties of the engineered soil and were found to be 0.2 and 0.0817, respectively. A characteristic moisture release curve was subsequently constructed in order to estimate volumetric moisture content of the soil at saturation and residual levels, for this soil found to be 0.57 and 0.038, respectively.

The runoff portion of the study presented in Chapter Two involved first the simulation of runoff for the study site in HYDRUS, based on rainfall and evapotranspiration measured or calculated from site-measured variables. Measured runoff at an adjacent site was used to validate HYDRUS derived values. Incorporating regression analysis, HYDRUS-1D was shown to provide accurate predictions for stormwater runoff with simulated versus observed runoff volume ($R^2 = 0.93$, slope = 1.3). Actual evapotranspiration, simulated in HYDRUS, was also

validated via a water balance calculation based on measured quantities of rainfall, runoff, and soil moisture changes. Regression analysis showed an R^2 of 0.88 and a slope of 0.99 for the comparison of simulated versus observed actual evapotranspiration.

With HYDRUS-1D runoff output validated, stormwater runoff for seven evaluation cities was simulated. Three additional engineered soil depths (five, fifteen and thirty cm) were simulated in addition to the ten cm of the study site greenroof system to assess the effect of soil depth on runoff. Runoff volume reduction compared to a conventional impervious roof ranged from 17-81 % for the evaluation cities. Average seasonal depth per rain event strongly affected the ability of greenroof systems to contain rainfall volume. The lowest volume reduction at 17 % culminated from simulations of a greenroof sited in Los Angeles, CA. where large rain events occurred in winter when evaporation potential was low resulting in relatively larger runoff volumes compared to other sites. The highest runoff reduction came from a greenroof simulation for Denver, CO., where the majority of rainfall (predominantly small events) fell in summer when evapotranspiration potential was high. Overall, simulations showed that greenroofs do reduce runoff greatly, and can be used in a comprehensive BMP to reduce urban stormwater runoff.

Aside from stormwater runoff prediction, essentially, the goal of the study involved deriving three input parameters for eQuest (Quick Energy Simulation Tool), the building energy modeling software. Required inputs included thermal conductivity, heat capacity, and surface absorptance. Chapter Three outlined the methods used to compute thermal conductivity and heat capacity of the engineered soil based on volumetric moisture content. Results showed that thermal conductivity exhibited little variation across the narrow range of moisture content witnessed at the study site and simulated in HYDRUS-1D. The narrow range of conductivity

simplified building energy modeling by providing one thermal conductivity input value (0.23 W m^{-1} $^{\circ}C^{-1}$) to be used for all evaluation cities.

Another input for eQuest, surface absorptance, was altered to include the effects of evapotranspiration, a quantity that would otherwise not be included in normal building energy simulations. Absorptance was calculated simply by adding latent heat flux to reflected radiation in the computation of surface reflectance. Results revealed that absorptance was reduced for all evaluation cities. An initial value of absorptance at 0.7 was assumed for the greenroof, which was merely an average of a light gray soil and a short grass. Evapotranspiration effects lowered absorptance from 0.7 to 0.67 at its highest (Phoenix, AZ) to the lowest value, 0.36 (Seattle, WA). Variation occurred mainly due to soil moisture available for evapotranspiration.

Once all input parameters were obtained, building energy loads were simulated for a variety of building designs. Initial simulation runs were made using eQuest for study site city, Athens, GA. For the Athens site, energy loads were simulated for three building heights each with two footprint shapes (at 929 m^2). The goal of simulating several building height was to determine how percent load reductions change with additional stories. In addition on each building, four roof types including a gravel-covered BUR, two cool roofs, and an extensive green roof were simulated. Percent load reductions compared the two cool roofs and the greenroof to a gravel-covered BUR. For square footprinted buildings, as building height increased, the percent reduction evident under the alternate roof types decreased. However, the trend was not so consistent for rectangular footprint shapes. For rectangular building footprint shapes, a change solar gain due to smaller southern exposure caused the difference in building energy loads compared to square footprint shapes. Greenroofs simulated for the Athens site exhibited energy load reductions in the range 0.1-5.0 % for cooling loads and –0.2-26 % for heating loads.

Additional simulations showed cooling and heating load reductions in the range of 2.5-6.9 % and –0.8-1.6 %, respectively, for a hypothetical ten-centimeter soil depth greenroof sited in the evaluation cities. The cool roof showed cooling load reductions in the range 4.3-8.0 % while heating loads actually increased by 0-11 %. Results also revealed that for a 10 cm greenroof in Seattle, WA, the energy load benefits when compared to a BUR would never repay the costs incurred for greenroof installation and replacement during the life of the building.

Overall, a successful stormwater runoff and energy load prediction tool was developed in the current research. Though many studies have developed prediction tools for stormwater runoff (Carter and Rasmussen, 2005; Moran et al, 2005), energy load prediction tools were not readily available to assess the energy saving benefits of greenroofs. In addition, a previously untested engineered soil was evaluated in term of hydraulic properties. In all, a method is presented with the hope that builders, designers, and planners could better predict for consumers the effects of greenroofs in various climate types long before construction begins at a site.

REFERENCES

Aber, J.D. and J.M. Melillo. 1991. *Terrestrial Ecosystems*. Philadelphia: Saunders College Publishing. 429pp

Allen, G.A., L.S. Pereira, D. Raes, and M. Smith. Crop Evapotranspiration: Guidelines for computing crop water requirements. *FAO Irrigation and Drainage Paper, No. 56.* 300pp

ASHRAE Handbook. 2001. *Fundamentals*. Atlanta: American Society of Heating, Refrigerating, and Air-Conditioning Engineers, Inc.

Booth, D. and C.R. Jackson. 1997. Urbanization of aquatics systems: Degradation thresholds, stormwater detention, and the limits of mitigation. Journal of the American Water Resources Association, 22(5): 1-20.

Campbell, G.S. 1985. *Soil Physics with Basic: Transport models for soil-plant systems*. Developments in Soil Science, 14. Amsterdam: Elsevier. 150pp

Carter, T. and T. Rasmussen. Use of greenroofs for ultra-urban stream restoration in the Georgia piedmont (USA). *Greening Rooftops for Sustainable Communities, proceedings.* May 2005, Washington D.C.

De Bruin, H.A.R. and A.A.M Holtslag. 1982. A simple parameterization of the surface fluxes of sensible and latent heat during daytime compared with the Penman-Monteith concept. Journal of Applied Meteorology, 21: 1610-1621

De Vries, D.A. 1966. Thermal Properties of Soils. *Physics of Plant Environment.* Ed. Van Wijk, W.R. Amsterdam; North-Holland Publishing Company. 382pp

Del Barrio, E. 1998. Analysis of the green roofs cooling potential in buildings. Energy and Buildings, 27: 179-193

Hargreaves, G., and Z. Samani. 1985. Reference crop evapotranspiration and temperature. Appl. Eng. Agri., 1(2): 96-99

Harrison, J. and L. Stribling. The urban environment and NPS pollution: Regulating urban stormwater runoff. Water quality: Controlling Nonpoint Source (NPS) Pollution. Alabama Cooperative Extension System, ANR-790-4.7.3.

Hilten, R. N., T. M. Lawrence, and E. W. Tollner. 2005a. Predicting stormwater runoff from a modular block greenroof system with engineered soil. To be submitted to the Journal of Hydrology.

Hilten, R. N., T. M. Lawrence, and E. W. Tollner. 2005b. Thermal conductivity of an engineered greenroof soil. To be submitted to the International Journal of Heat and Mass Transfer.

Krischer, O. and H. Rohnalter. 1940. Warmeleitung and dampfdiffusion in feuchten Gutern. V.D.I. Forschungsheft 402.

Markham, J. and T. Walles. 2003. Making green roofs simple. Environmental Design and Construction. Available online at: http://www.edcmag.com.

McInnes, K.J. 1981. Thermal conductivities of soils from dryland wheat regions of Eastern Washington. M.S. Thesis, Washington State University, Pullman

Moran, A., B. Hunt and J. Smith. Hydrologic and water quality performance from greenroofs in Goldsboro and Raleigh, North Carolina. *Greening Rooftops for Sustainable Communities, proceedings.* May 2005, Washington D.C.

Monteith, J.L. 1965. Evaporation and the environment. Sym. Soc. Exp. Biol., 19: 205-234

NCDC. 2004. The National Climatic Data Center. Available online at: http://www.ncdc.noaa.gov.

Niachou, A., K. Papakonstantinou, M. Santamouris, A. Tsangrassoulis, G. Mihalakakou. 2001. Analysis of the green roof thermal properties and investigation of its energy performance. Energy and Buildings, 33: 719-729

Paul, M., and J. Meyer. 2001. Streams in the urban landscape. Annual Review of Ecological Systems, 32: 333-365

Penman, H.L. 1948. Natural evaporation from open water, bare soil, and grass. Proc. Roy. Soc. London, A193: 120-195

Philip J.R. and D.A. De Vries. 1957. Moisture movement in porous materials under temperature gradients. Transactions, American Geophysical Union, 38(2): 222-232

Pielke, R. Jr. 2002. *Mesoscale Meteorological Modeling.* San Diego: Academic Press. 676pp

Prowell, E. Runoff quantities for a modular block greenroof system. Personal communication.

Schaap, M.G., F.J. Leij, and M. Th. van Genuchten. 2001. Rosetta: a computer program for estimating soil hydraulic parameters with hierarchical pedotransfer functions. Journal of Hydrology, 251: 163-176

Šimůnek, J., M. van Genuchten, and M. Sejna. Code for simulating the one-dimensional movement of water, heat and multiple solutes in variably saturated porous media. US Salinity Laboratory, USDA

Theodosiou, Theodore G. 2003. Summer period analysis of the performance of a planted roof as a passive cooling technique. Energy and Buildings, 35: 909-917

Vershinin, P.V. 1966. Fundamentals in agrophysics. Ioffe, A.F. and I.B. Revut (eds), Israel Program for Scientific Translations.

van Genuchten, M. Th. 1980. A closed-form equation for predicting the hydraulic conductivity of unsaturated soils. Soil Sci. Am. J., 44: 892-898

Wong, N. H., Y. Chen, C. L. Ong, and A. Sia. 2003. Investigation of thermal benefits of rooftop gardens in the tropical environment. Building and Environment, 38: 261-270